ANSTO/E-777

Australian Government

Nuclear-based science benefiting all Australians

Contour plots of New South Wales Fine Particle Measurements at Seven Sites between 1998 and 2012.

by

J. Crawford

D. D. Cohen

Prepared within the Institute for Environmental Research
Australian Nuclear Science and Technology Organisation

February 2013

Abstract

Under the ANSTO Aerosol Sampling Program (ASP), $PM_{2.5}$ samples were collected at seven sites in NSW, Australia, since 1998. The elemental composition of each sample was determined using IBA techniques, after which positive matrix factorisation (PMF) analysis was carried out to obtain a set of source fingerprints and their concentrations for each of the sites.

Spatial interpolation of elemental concentrations as well as PMF source fingerprints was carried out using the kriging interpolation technique. The spatial concentration maps generated provided an indication of which regions received higher $PM_{2.5}$ concentrations, which also varied with season. For example higher concentrations of BC and K occurred in winter, whereas, in summer the concentrations of sea salt were higher. The two inland sites, Richmond and Muswellbrook, received the least salt, although, there were sampling days on which higher concentrations of salt were measured at the inland site than the coastal site, indicating sources of salt other than the ocean.

Keywords: $PM_{2.5}$, New South Wales, aerosols

ISSN **10307745**
ISBN **1 921268 18 2**

Contents

List of Figures

List of Tables

1 Introduction

Under the ANSTO Aerosol Sampling Program (ASP), $PM_{2.5}$ samples have been collected at a number of sites in NSW, Australia (Figure 1, Table 1). Given that there is a limit to the number of sampling sites, as resources are needed for setting up and maintaining a sampling site and then analysing the samples, it is common practice to use some method of determining the likely concentrations at neighbouring locations where sampling has not be undertaken. One technique commonly in use is the spatial interpolation of monitoring data (Wong et al., 2004, Horálek et al., 2008). Although, modelling data and supplementary data can also be used (Horálek et al., 2008).

In this study monitoring data, for 7 sites in NSW, was used in a spatial interpolation scheme. Interpolation was carried out on elemental concentrations as well as the concentration of identified source fingerprints. For the elemental concentrations monthly average values from January 2007 to December 2011 were used. For the source fingerprints daily concentrations since 1998 were used and only for those days on which measurements were available at all 7 sites.

Airborne particulate matter and in particular $PM_{2.5}$ has been associated with human health risks (Dockery et al., 1993, Russell and Brunekreef, 2009, Schwartz et al., 2000). Thus knowledge of the concentrations that the population is exposed to is of particular importance. The seven sampling sites are located in the more populated regions along the coast of New South Wales and thus the interpolated values closer to the measurement sites, which are likely to be more representative of the true concentrations, account for a larger population than those concentrations further west which may be less representative of the true concentrations (due to the extrapolation).

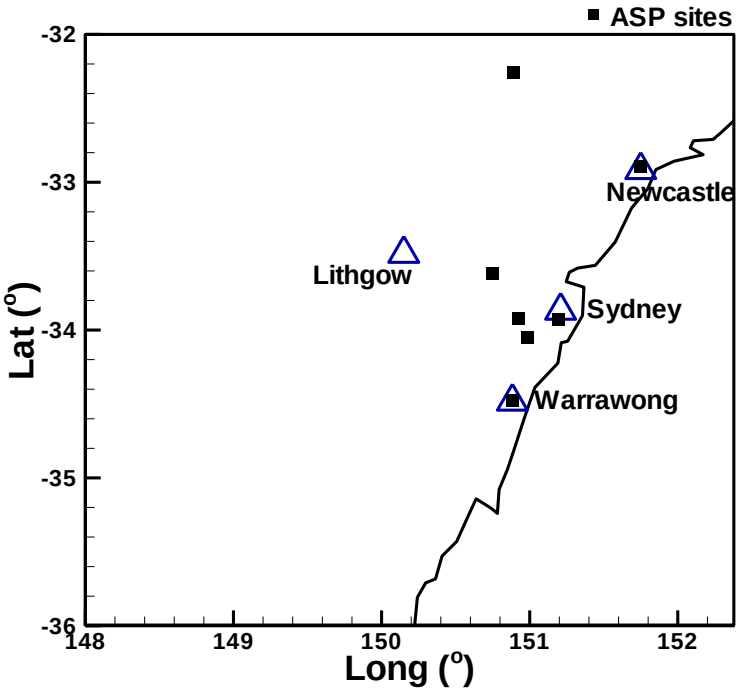

Figure 1: Location of sampling sites.

Table 1: Sampling sites and their coordinates.

	Long (x)	Lat (y)
Liverpool	150.92	-33.93
Muswellbrook	150.89	-32.26
Mascot	151.20	-33.93
Richmond	150.75	-33.62
Warrawong	150.88	-34.48
Mayfield	151.75	-32.90
Lucas Heights	150.98	-34.05

2 $PM_{2.5}$ sampling and elemental analysis

The aerosol sampling program constituted 24-hour integrated samples (from midnight to midnight local time) taken twice a week (Wednesday and Sunday) using a cyclone $PM_{2.5}$ system with 22 l/min flow rate (Cohen et al., 1996).

Accelerator-based ion beam analysis (IBA) techniques were used to perform the elemental analyses of the aerosol samples (Cohen, 1998; Cohen et al. 2004). These techniques can provide quantitative elemental information on a broad range of elements including: H, Na, Al, Si, P, S, Cl, K, Ca, Ti, V, Cr, Mn, Fe, Co, Ni, Cu, Zn, Br, Pb. The full suite of analyses included: Proton-induced X-ray Emission (PIXE), Proton-induced Gamma-ray Emission (PIGE), Rutherford Backscattering (RBS) and Proton Elastic Scattering Analysis (PESA). Laser absorption methods were used to determine the black carbon (BC) concentrations (Cohen et al., 2000, and Taha et al., 2007).

From the determined elemental concentrations estimates of ammonium sulfate, soil and sea salt were made according to Malm et al., (1994):

$$\text{Salt} = 2.54[\text{Na}] \quad (1)$$

$$\text{Ammonium Sulfate} = 4.125[\text{S}] \quad (2)$$

$$\text{Soil} = 2.20[\text{Al}] + 2.49[\text{Si}] + 1.63[\text{Ca}] + 1.94[\text{Ti}] + 2.42[\text{Fe}] \quad (3)$$

$$\text{Smoke estimate} = [\text{K}] - 0.6[\text{Fe}] \quad (4)$$

$$\text{Organics} = 11[\text{H}] - 0.25[\text{S}] \quad (5)$$

$$\text{RCM} = \text{Salt} + \text{Ammonium Sulfate} + \text{Soil} + \text{Smoke} + \text{Organics} + \text{BC} \quad (6)$$

where the [ ] represent the concentration of that element. In equation (2) the assumption is that the entire sulfate is fully neutralised and occurs on the filter as ammonium sulfate. In equation (5), the organic matter estimate, the assumption is that the average $PM_{2.5}$ organic composition was 9%H, 20%O and 71%C (Malm et al., 1994).

Once the concentrations were determined, monthly average concentrations were calculated for each month of each year. The mean, median, standard deviation and

maximum of the monthly average concentrations, for January 2007 to December 2011, are presented in Table 2. Lucas Heights shows the lowest median $PM_{2.5}$ mass concentration, although the maximum is higher than that for Warrawong. The highest Salt was recorded at Warrawong and Mascot, which is consistent with these two sites located closer to the ocean.

Table 2: Statistics for each of the sites for the total mass and for selected elements in ng/m^3.

	Warrawong				Lucas Heights				Mascot			
	Mean	Median	SD	Max	Mean	Median	SD	Max	Mean	Median	SD	Max
Mass	6665	6132	3267	24369	5492	4933	3783	32044	8202	7084	5453	46632
$(NH_4)_2SO_4$	1933	1779	946	4641	1523	1352	668	3137	1605	1480	562	2873
Organ.	523	422	474	2417	624	490	612	4228	1792	1045	3039	22851
Soil	807	636	989	7766	424	249	1136	8915	664	470	1291	10170
Elt. C.	711	704	168	1122	562	565	135	792	1311	1109	562	2666
Salt	1037	1043	598	2630	777	736	505	2429	1038	988	622	3017
K	52	42	36	295	39	31	43	357	58	50	54	438
Fe	185	162	147	999	52	31	152	1201	109	72	195	1546
Zn	28	23	16	88	6	6	3	13	14	10	10	48
Pb	7	6	4	23	2	2	1	5	13	9	14	65
	Liverpool				Richmond							
	Mean	Median	SD	Max	Mean	Median	SD	Max				
Mass	8505	6951	5264	43644	7101	5921	5461	45484				
$(NH_4)_2SO_4$	1635	1414	678	3229	1499	1363	685	2860				
Organ.	2055	1429	2123	11949	2565	1072	7257	56779				
Soil	647	428	1261	9979	463	232	1351	10616				
Elt. C.	1344	1125	545	2823	739	665	291	1590				
Salt	739	638	537	2532	474	406	374	1758				
K	74	58	58	425	64	46	62	449				
Fe	96	68	180	1446	56	26	213	1673				
Zn	15	12	9	38	6	6	3	14				
Pb	6	5	5	19	5	4	4	18				
	Mayfield				Muswellbrook							
	Mean	Median	SD	Max	Mean	Median	SD	Max				
Mass	7591	6435	6687	57267	6476	5299	5737	48347				
$(NH_4)_2SO_4$	1499	1476	523	2735	1540	1373	670	2969				
Organ.	1994	849	7129	55963	2273	917	9156	71799				
Soil	754	522	1101	8770	814	509	1514	10967				
Elt. C.	1048	987	290	1924	720	705	223	1243				
Salt	984	810	604	3097	390	321	305	1363				
K	53	46	44	369	47	38	53	417				
Fe	106	80	164	1310	76	39	222	1726				
Zn	21	15	21	134	3	3	3	13				
Pb	6	5	5	26	3	2	2	12				

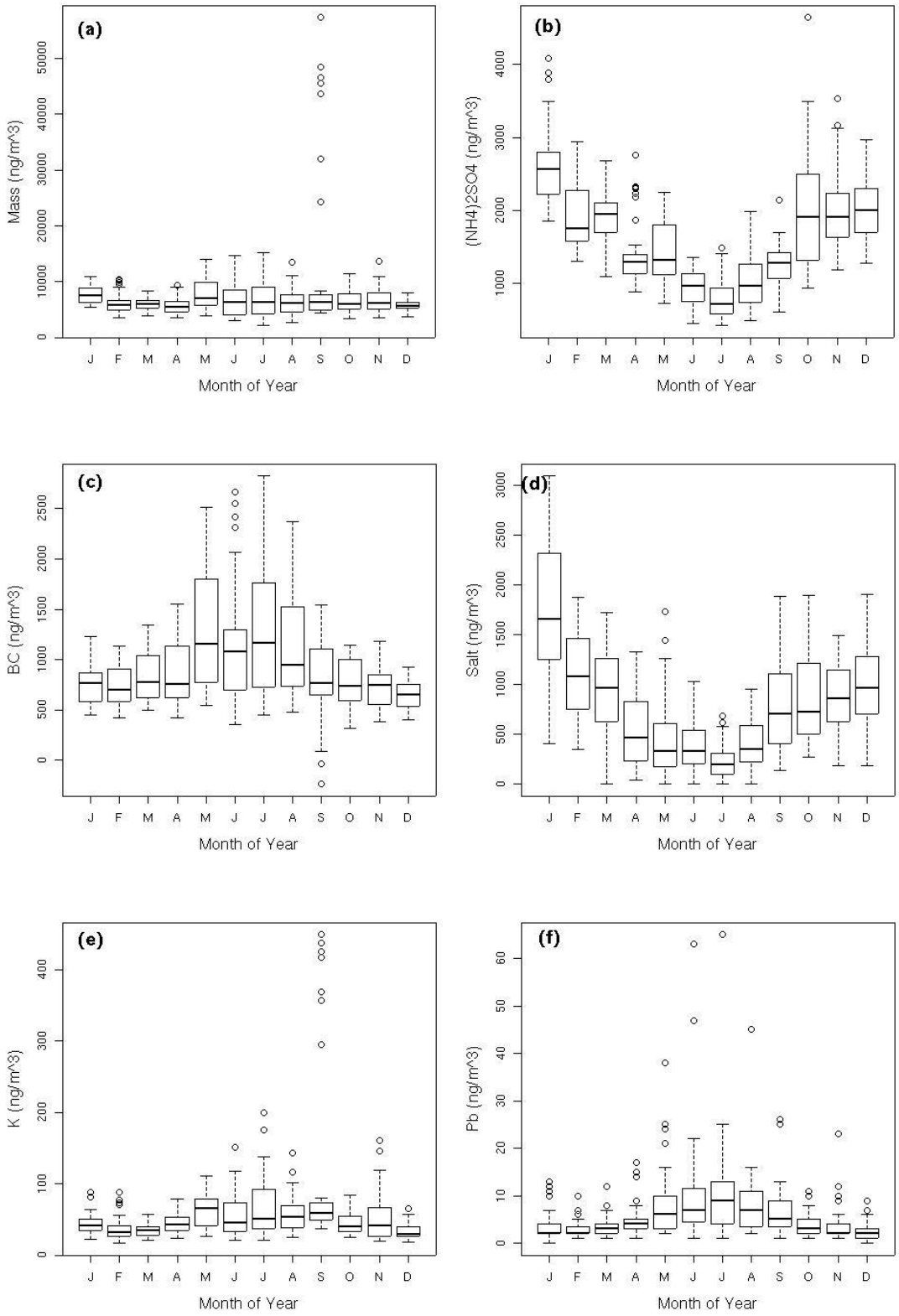

Figure 2: Box and whisker plots of monthly average concentrations of (a) Mass, (b) $(NH_4)_2SO_4$, (c) CB, (d) Salt, (e) K and (f) Pb. Boxes represent 25 – 75% percentile, the median is represented by the line through the box, the top and bottom 25% are represented by the whiskers with some outliers presented by the open circles.

Box and whisker plots of monthly average concentrations, from all sites, are presented in Figure 2. A clear seasonal trend is present in all cases, with a higher concentration in winter for $PM_{2.5}$ Mass, BC, K and Pb and a higher concentration in summer for $(NH_4)_2SO_4$ and Salt. This is consistent with their sources, for example BC and K are markers for smoke (Cohen et al., 2012) which were higher in winter due to domestic use of firewood for heating. The $(NH_4)_2SO_4$ concentrations were higher in summer due to more suitable conditions for the reaction of SO_2 with ammonium. Whereas Salt was higher in summer as the prevailing wind directions in summer are from the north-east to south-east quadrant and sea breezes are more common in summer, thus more sea spray would be present in the summer air. For the $PM_{2.5}$ Mass and for K some outliers were present in September, which were due to a severe dust storm in September 2009.

3 Source fingerprints

The PMF2 program (Paatero 2010) was used to identify sources contributing to the $PM_{2.5}$ measured at each site. In this report we consider the following sources:

- *PMFMass* being the sample mass as approximated by the positive matrix approximation (PMF) technique.
- *2ndryS* for secondary sulfate formed from reactions of SO_2 with ammonium in the atmosphere,
- *Auto* for emissions from motor vehicles,
- *Smoke* for smoke emissions
- *Sea* for fresh sea salt
- *Soil* for soil dust, and
- *Ind* for emissions from industry

The fingerprints for Richmond and their seasonal distribution were detailed in Cohen et al., (2012) and those for Liverpool were detailed in Cohen et al. (2011). Box and whisker plots of the concentrations are presented for each of the sites in Figure 3. Higher median concentrations of PMF Mass were present at Liverpool, closely followed by Mascot and Mayfield. For secondary sulfate (*2ndryS*) a large range is seen at the industrial site, Warrawong. Higher median concentrations of the *Smoke* fingerprint were present at Richmond, Mascot and Mayfield. The lowest fresh sea spray concentrations were recorded for the inland sites, Richmond and Muswellbrook.

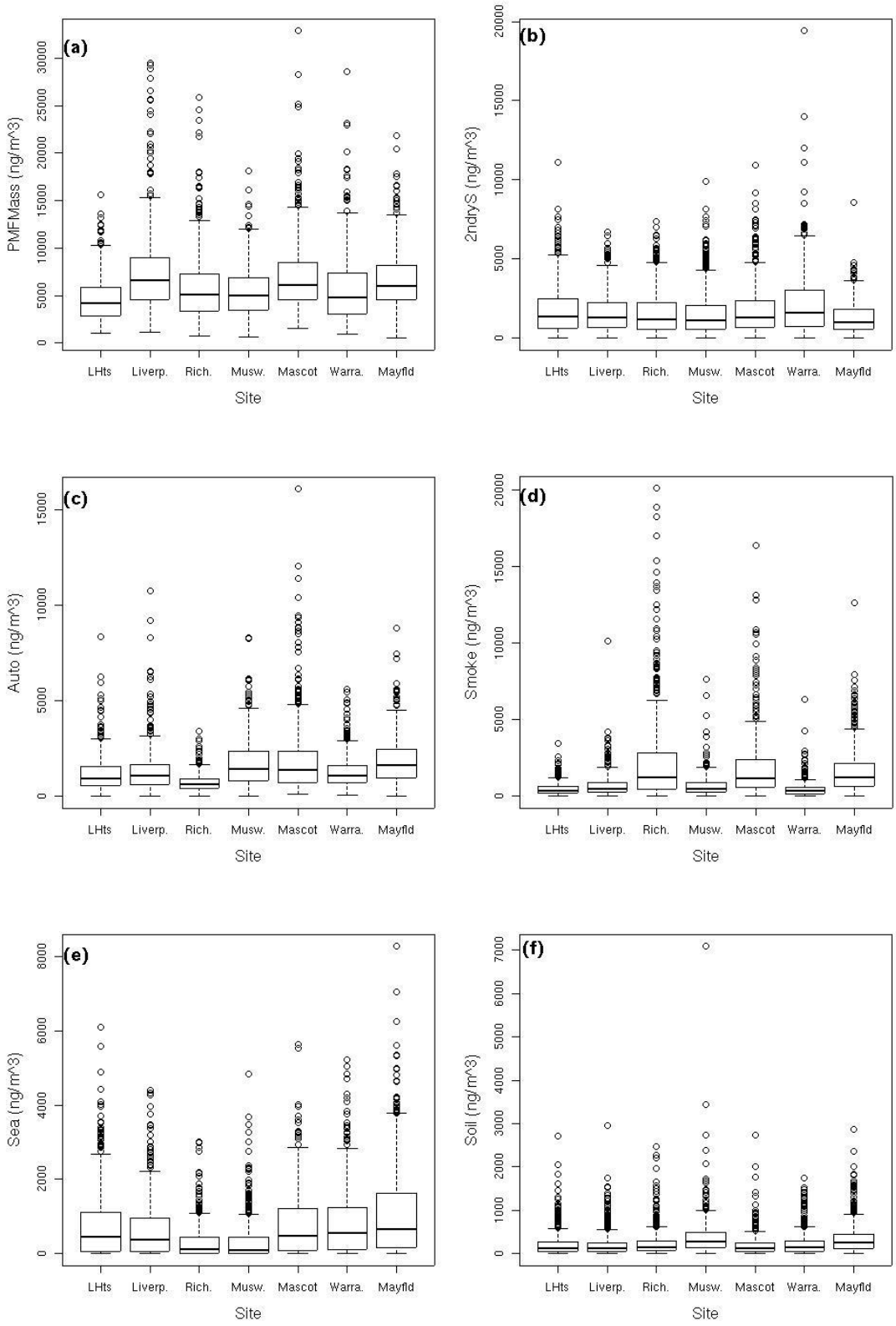

Figure 3: Box and whisker plots of concentrations (for Lucas Heights, Liverpool, Richmond, Muswellbrook, Mascot, Warrawong and Mayfield) of (a) PMFMass, (b) *2ndryS fingerprint*, (c) *Auto fingerprint*, (d) *Smoke fingerprint*, (e) *Sea fingerprint* and (f) *Soil fingerprint*. Boxes and whiskers, as for Figure 2.

4 Spatial interpolation

Wong et al. (2004) compared the results of spatial interpolation of air quality data using four methods; spatial averaging, nearest neighbour, inverse distance weighted and kriging. They found that the different methods did not produce dramatically different estimates where the monitoring sites density was relatively low. However, substantial differences were found between the results produced by the different interpolation methods when the density of sampling sites was relatively high. A summary of each technique is presented in their paper.

5 Spatial interpolation for NSW $PM_{2.5}$ data

Seven sampling sites were available for the NSW region. Monthly average $PM_{2.5}$ concentrations were used from January 2007 to December 2011 to produce concentration maps, one for each month (i.e. a total of 60 maps). Also daily fingerprint estimates were used to generate daily fingerprint concentrations maps since July 1998.

A bounding box of 8°x8° was defined with Sydney (located at 151.2086°E, 33.8683°S) being in the centre of the box. Then spatial interpolation was carried out over the region defined by the box. Given that only seven sites were available for the interpolation and effectively an extrapolation was being obtained further form these monitoring locations, on the boundary of the box, the values were set to the data set median values divided by 10. The boundary was chosen such that it had small impact on interpolated values close to the locations where measurements were available.

In this application, kriging, as implemented in the Tecplot software package (Tecplot, 2003), was used to obtain contour maps of the $PM_{2.5}$ total mass concentrations, elemental concentrations and identified source fingerprints. For the kriging the range was set to 0.2 which resulted in sites being significant if they were no more than 2.25 degrees from the point whose value was to be determined (i.e. at a distance of 2.25 degrees or ~ 225km).

The interpolation was carried out in the long, lat coordinate system, following which a transformation of the coordinates was carried out to obtain the distance from Sydney in km.

In the Appendices the concentration maps generated (after the interpolation by kriging was carried out) for $PM_{2.5}$ total mass concentration and the concentrations for a selected set of elements is presented. When analysing the maps one needs to keep in mind that the interpolated concentrations are only significant close to the monitoring sites.

The seasonal concentrations are evident in the concentrations maps, although the variability within seasons is also evident. For example a high concentration of $PM_{2.5}$ mass was seen at all sites in January of 2007 but much lower concentrations were seen in February of the same year (Figure 10). The sea salt concentration is higher at the coastal sites and also higher during the warmer months of the year when sea

breezes are more prevalent, although, there was sampling days on which higher concentrations of salt were measured at the inland site than the coastal site, indicating sources of salt other than the ocean.

At a number of times over the 5 years much higher concentrations of $(NH_4)_2SO_4$ are recorded at Warrawong.

6 Spatial interpolation for NSW $PM_{2.5}$ PMF source fingerprints

Spatial interpolation of the PMF derived source fingerprints was undertaken on a daily basis for those days on which samples were available from all seven sites. A total of 554 concentration maps were generated for each source fingerprint from July 1998 to June 2012. Thus, these are not reproduced in this report; however, a few have been selected for discussion in the following sections.

6.1 PMF Sea Salt fingerprint

The *Sea* PMF fingerprint contour map for 14th of Dec 2011 is presented in Figure 4. A concentration of 2µg/m^3 or more was recorded along the coast and extending inland consistent with summer sea breezes carrying moist oceanic air inland. Compare to the winter concentrations (Figure 5) of less than 1µg/m^3, when the prevailing winds are from the south and south-west over land.

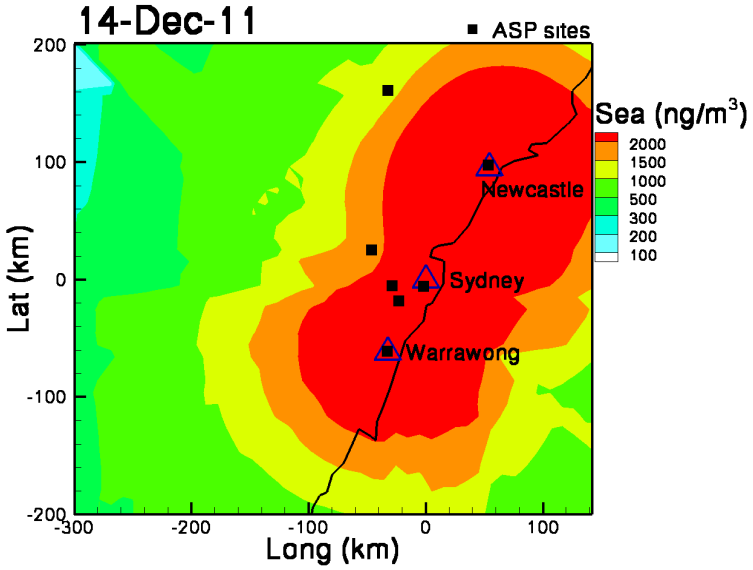

Figure 4: PMF *Sea* fingerprint contour map for 14th Dec 2011.

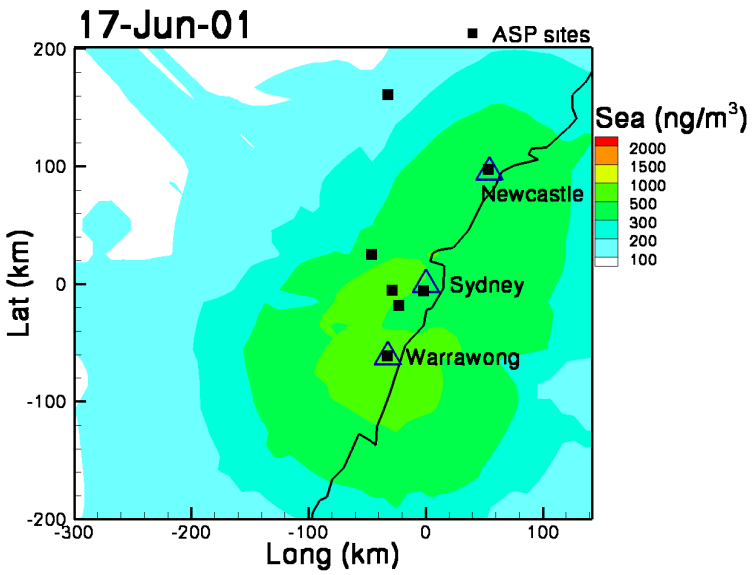

Figure 5: PMF *Sea* fingerprint contour map for 17th Jun 2001.

6.2 Comparison between contour maps of K and the Smoke fingerprint

K is one of the key elements in the *Smoke* fingerprints. In the following figures (Figure 6 and Figure 7) we present the monthly average K concentration for June 2008, followed by the estimated concentration of the PMF identified *Smoke* fingerprint for the five days of measurement. Note the similarity in the spatial extent of higher K and also higher values for the *Smoke* fingerprint. The highest concentration of the *Smoke* fingerprint is seen at Richmond in winter (see also Figure 3). For example on the 29th of June 2008 the concentration of the PMF *Smoke* fingerprint was higher than 10μg/m^3. This is a period when fire wood is used for domestic heating. However, a variation within the month is seen (Figure 7) which perhaps could be as a result of the prevailing meteorological conditions.

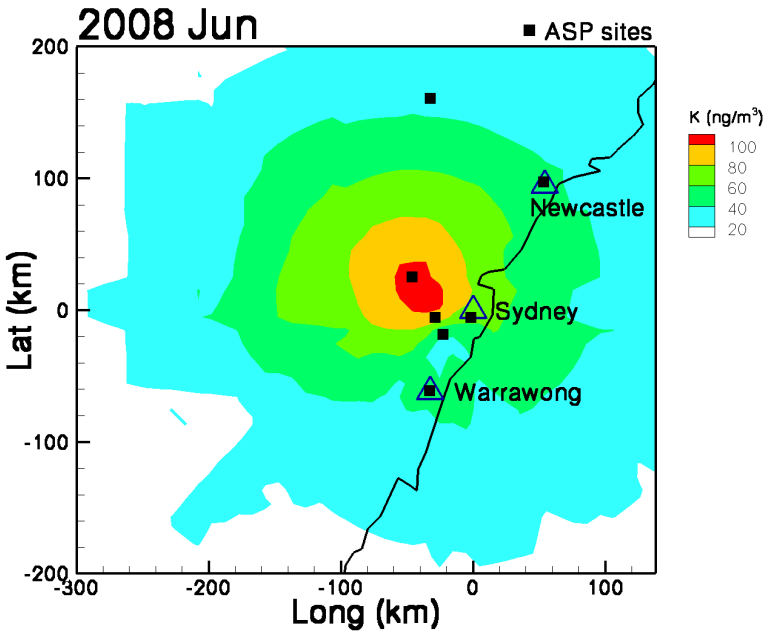

Figure 6: Average concentration of element K for June 2008.

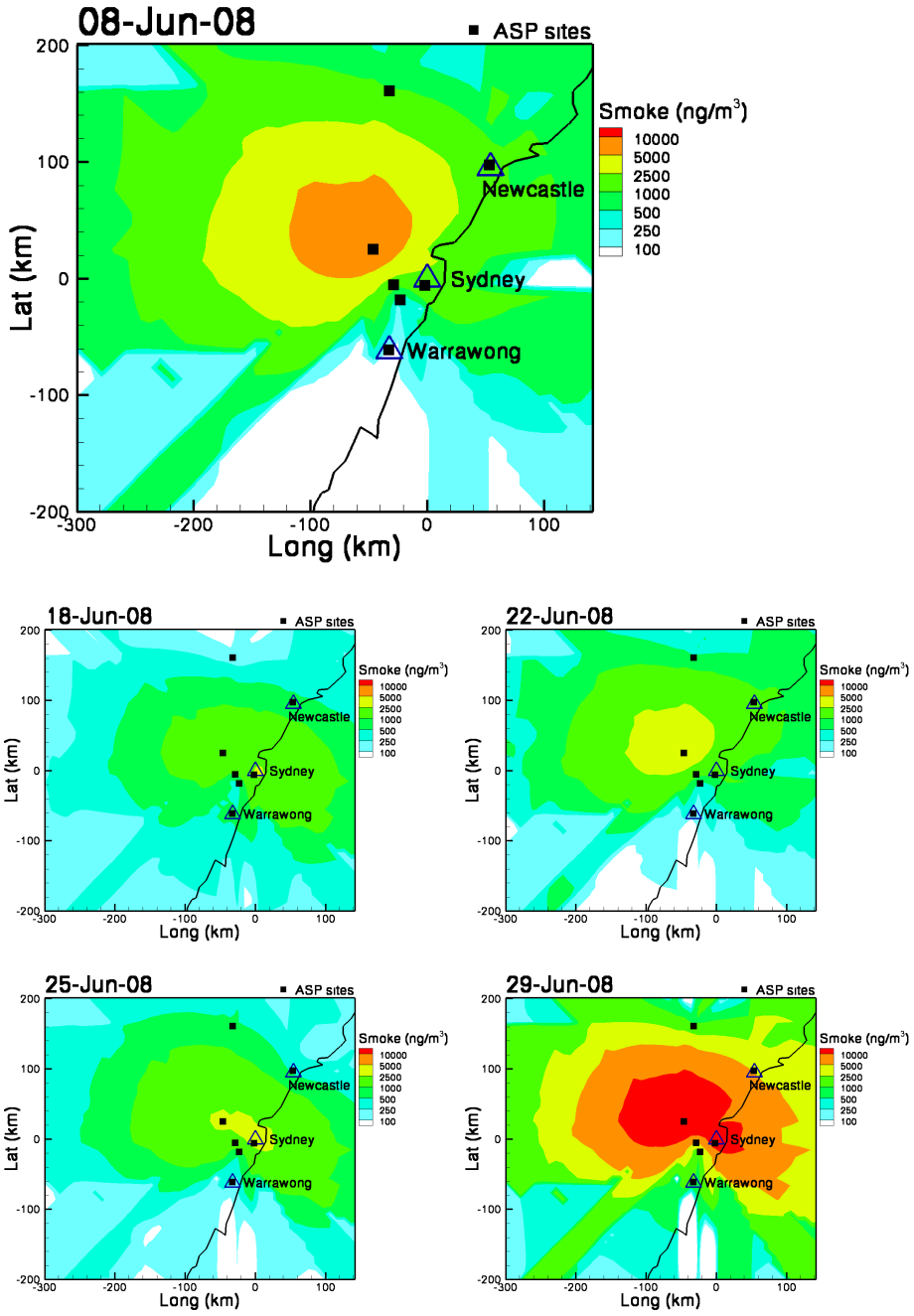

Figure 7: Concentration of the PMF *Smoke* fingerprint for Jun 2008.

6.3 PMF secondary sulfate (2ndryS) fingerprint

From Figure 3 we see that higher concentrations of the secondary sulfate fingerprint can occur at Warrawong when compared to the other sites. At Warrawong the $PM_{2.5}$ sampling is conducted close to a steel production industrial complex which is the most likely contributor to the higher secondary sulfate observed at this site (Figure 8). However, the concentration of secondary sulfate is more variable over the region; see for example Figure 9, where higher concentrations are also seen at Muswellbrook (located close to two power stations) and Mascot (located close to the Sydeny CBD). These maps provide a good visual indication of which regions are more likely to be exposed to higher concentrations.

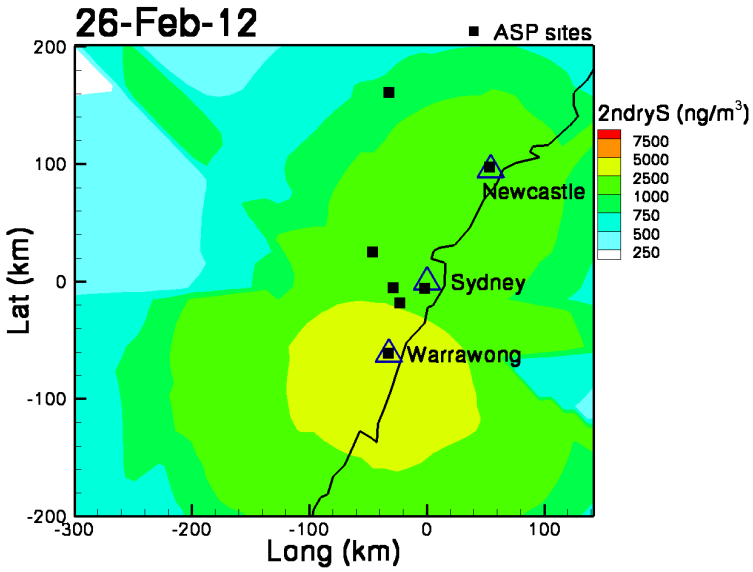

Figure 8: Concentration of the PMF secondary sulfate (*2ndryS*) fingerprint for 26th of Feb 2012.

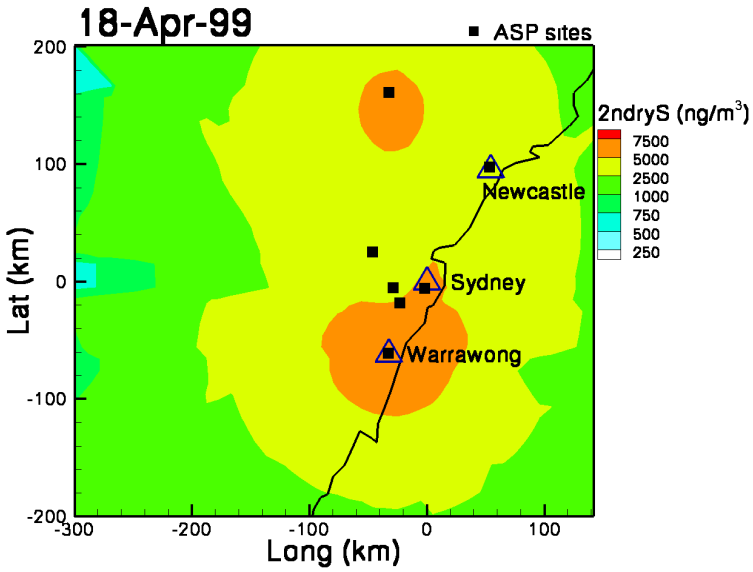

Figure 9: Concentration of the PMF secondary sulfate (*2ndryS)* fingerprint for 18th of Apr 1999.

7 Conclusions

$PM_{2.5}$ sampling was undertaken at seven sites in New South Wales, following which the elemental concentrations for each sample was determined using IBA techniques. A seasonal pattern in the concentrations was present with BC and K having higher concentrations in winter, whereas, higher concentrations of Sea Salt occurring in summer. PMF analysis was also carried out to obtain a set of source fingerprints and their concentrations for each of the sites.

Spatial interpolation of the concentrations was carried out using the kriging interpolation technique. The spatial concentration maps so generated provide an indication of which regions received higher $PM_{2.5}$ concentrations, which varied with the time of year. Higher concentrations of salt were seen at the coastal sites, although on occasions higher concentrations were seen in the inland sites to those at the coastal sites on the same day (e.g. 16th Sep 1998), indicating other sources of salt.

These maps can be used to provide average PM2.5 concentrations over large areas of NSW over many years useful for modellers.

8 References

Cohen D.D., Bailey G.M. and Kondepudi R., 1996: Elemental analysis by PIXE and other IBA techniques and their application to source fingerprinting of atmospheric fine particle pollution, Nucl. Instr. and Methods 109, 218-226.

Cohen D.D., 1998: Characterisation of atmospheric fine particles using IBA techniques. Nuclear Instruments and Methods in Physics Research B136-B138, 14-22.

Cohen D.D., Taha G., Stelcer E., Garton D., Box G., 2000: The Measurement and Sources of Fine Particle Elemental Carbon at Several Key Sites in NSW over the Past Eight Years. 15th International Clean Air Conference, Sydney Australia.

Cohen D.D, Garton D., Stelcer E., Hawes O., 2004: Accelerator based studies of atmospheric pollution processes. Radiation Physics and Chemistry 71, 758-567.

Cohen D.D., Stelcer E., Garton D., Crawford J., 2011. Fine particle characterisation, source apportionment and long-range dust transport into the Sydney Basin: a long term study between 1998 and 2009. Atmospheric Pollution Research 2, 182-189.

Cohen D.D., Crawford J., Stelcer E., Atanacio A.J., 2012. Application of positive matrix factorization, multi-linear engine and back trajectory techniques to the quantification of coal-fired power station pollution in metropolitan Sydney. Atmospheric Environment, 61, 204-211.

Dockery, D.W., Pope III., C.A., Xiping, X., Spengler, J.D.,Ware, J.H., Fay, W.E., Ferris Jr., B.G., Speiser, F.E., 1993. An association between air pollution and mortality in six US cities. New England Journal of Medicine 329, 1753–1759.

Hengl T. 2007: A Practical Guide to Geostatistical Mapping of Environmental Variables. EUR 22904EN – 2007.

Horálek J., De Smet P., De Leeuw F., Denby B., Kurfürst P., Swart R. European air quality maps for 2005 including uncertainty analysis. ETC/ACC Technical Paper 2007/7 March 2008.

Malm, W.C., Sisler, J.F., Huffman, D., Eldred, R.A., Cahill, T.A., 1994. Spatial and seasonal trends in particle concentrations and optical estimations in the US. J. Geophys. Res. 99, 1347-1370.

Paatero P., 2010. User's Guide for Positive Matrix Factorisation programs PMF2 and PMF3, Parts 1 and 2.

Russell A.G, Brunekreef B., 2009. A Focus on Particulate Matter and Health. Environmental Science and Technology Feature, 43, 4620-4625.

Schwarts J., Dockery D.W., Neas L.M., 1996. Is daily mortality associated specifically with fine particles? J. Air & Waste Management Association, 46, 927-939.

Taha G., Box G.P., Cohen D.D, Stelcer E., 2007: Black Carbon Measurement using Laser Integrating Plate Method. Aerosol Science and Technology, 41, 266-276.

Tecplot 2003. Tecplot User's Manual, Version 10. Amtec Engineering, Inc. Bellevue, Washington.

Wang D.W., Yuan L., Perlin S.A., 2004: Comparison of spatial interpolation methods for the estimation of air quality data. Journal of Exposure Analysis and Environmental Epidemiology, 14, 404-415.

Appendix 1: PM2.5 concentration maps

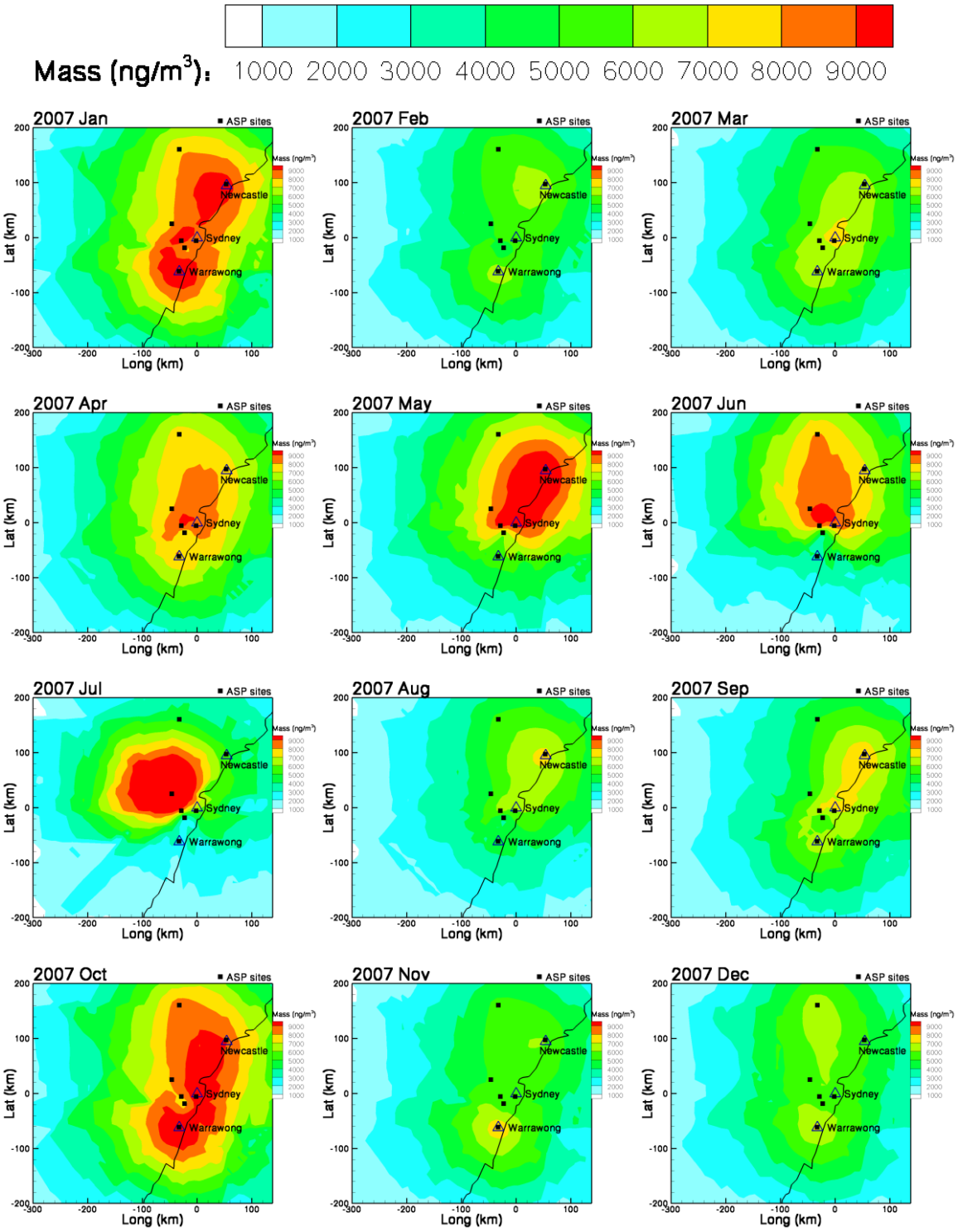

Figure 10: Contour maps of monthly average $PM_{2.5}$ mass concentration for 2007.

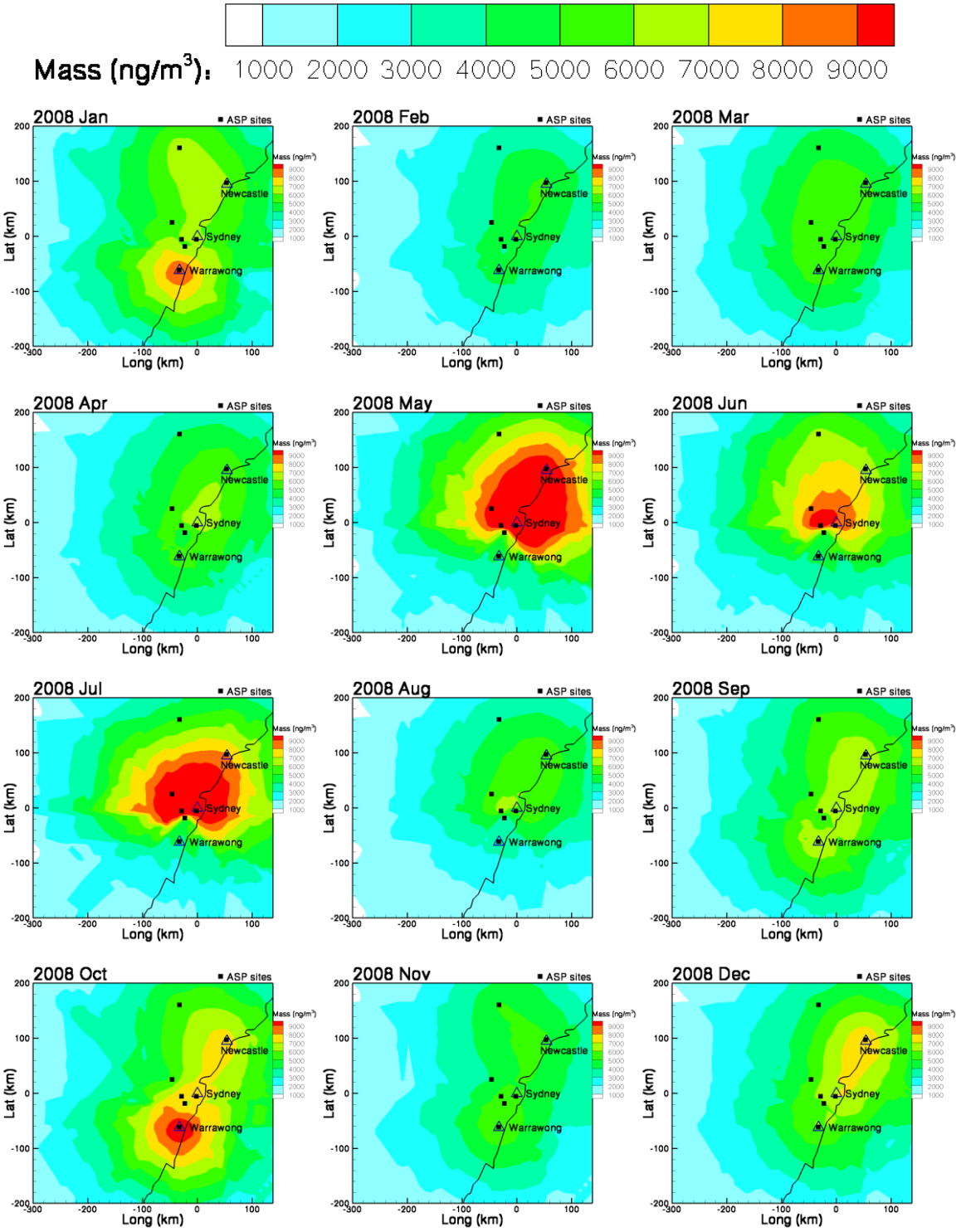

Figure 11: Contour maps of monthly average $PM_{2.5}$ mass concentration for 2008.

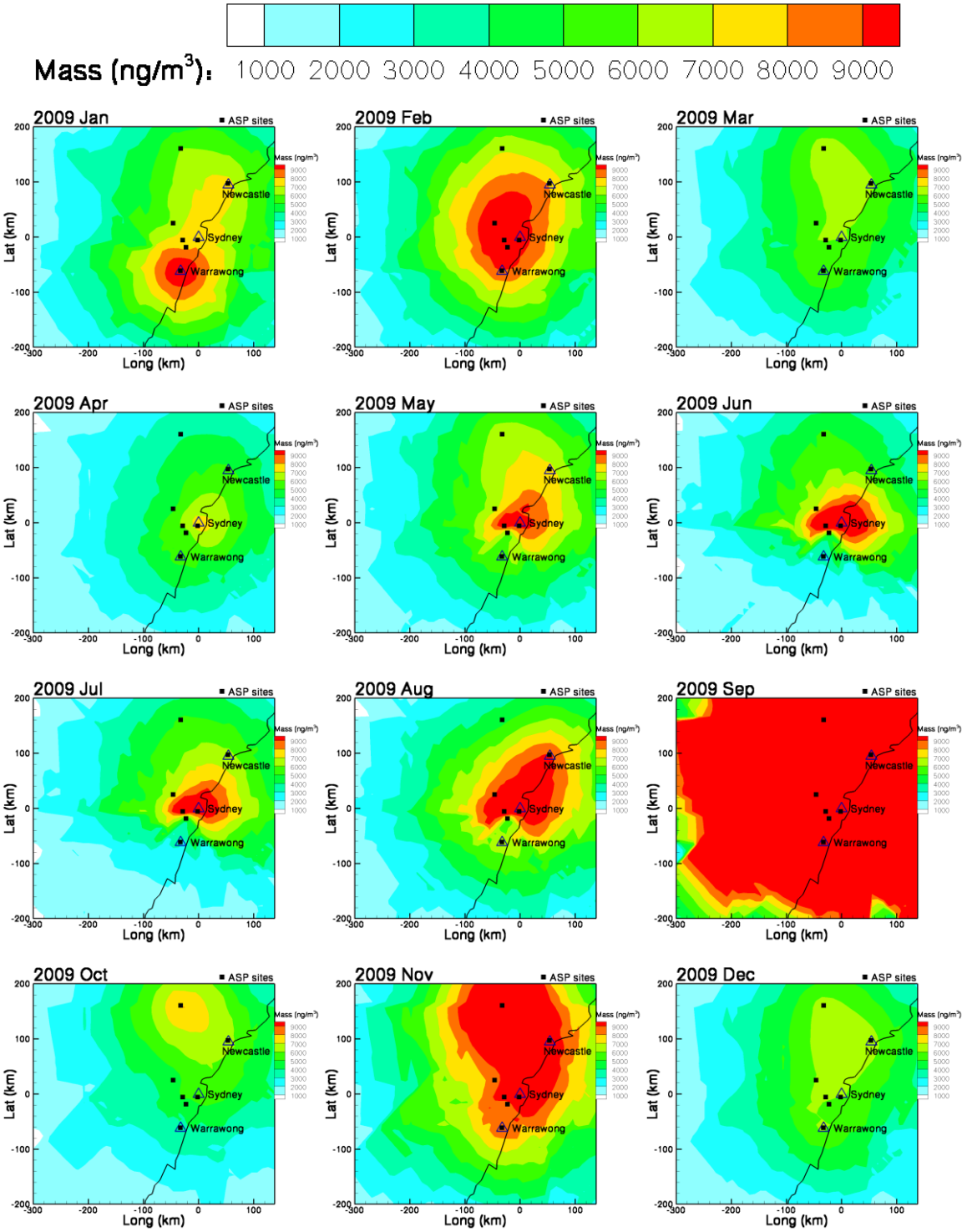

Figure 12: Contour maps of monthly average $PM_{2.5}$ mass concentration for 2009.

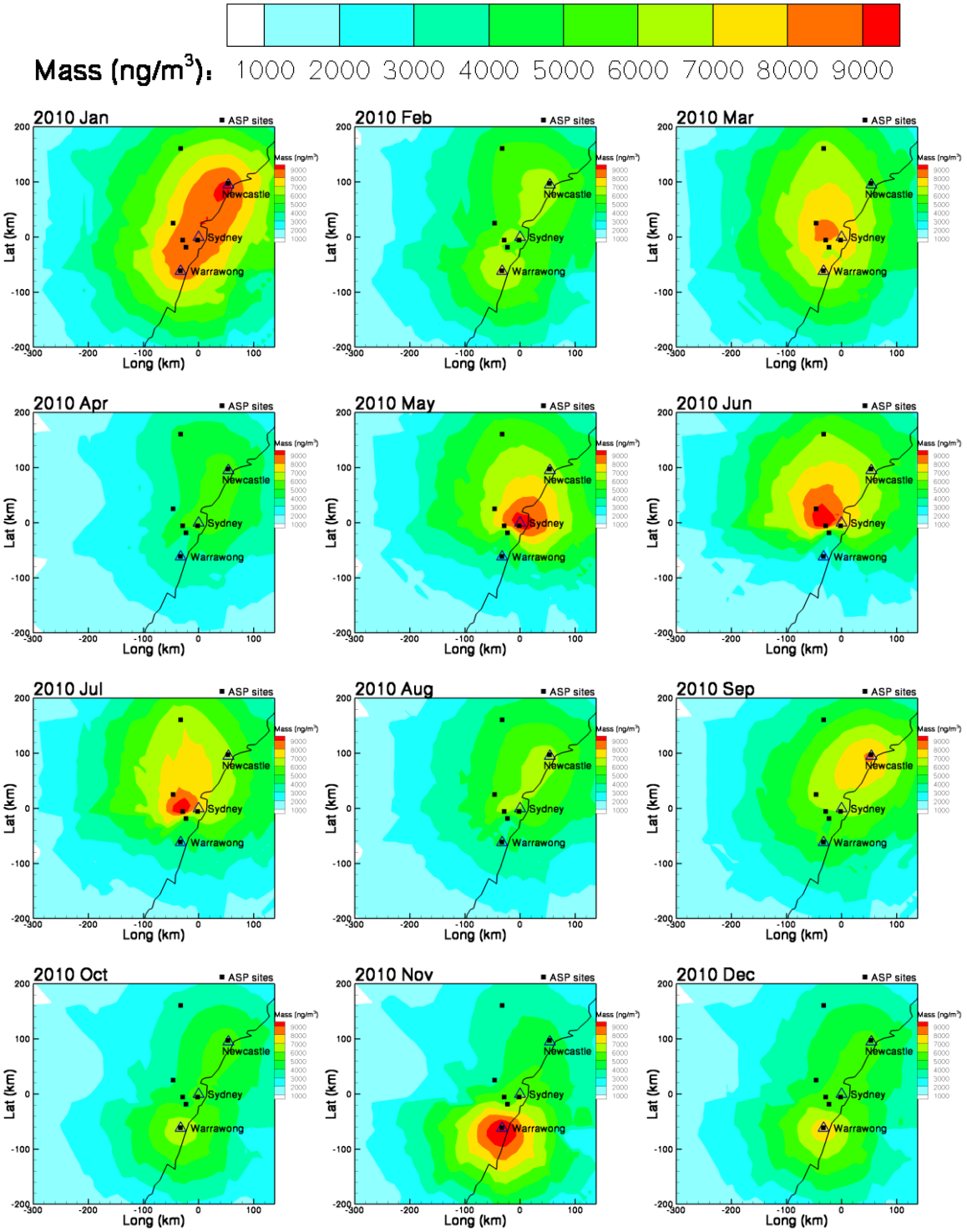

Figure 13: Contour maps of monthly average $PM_{2.5}$ mass concentration for 2010.

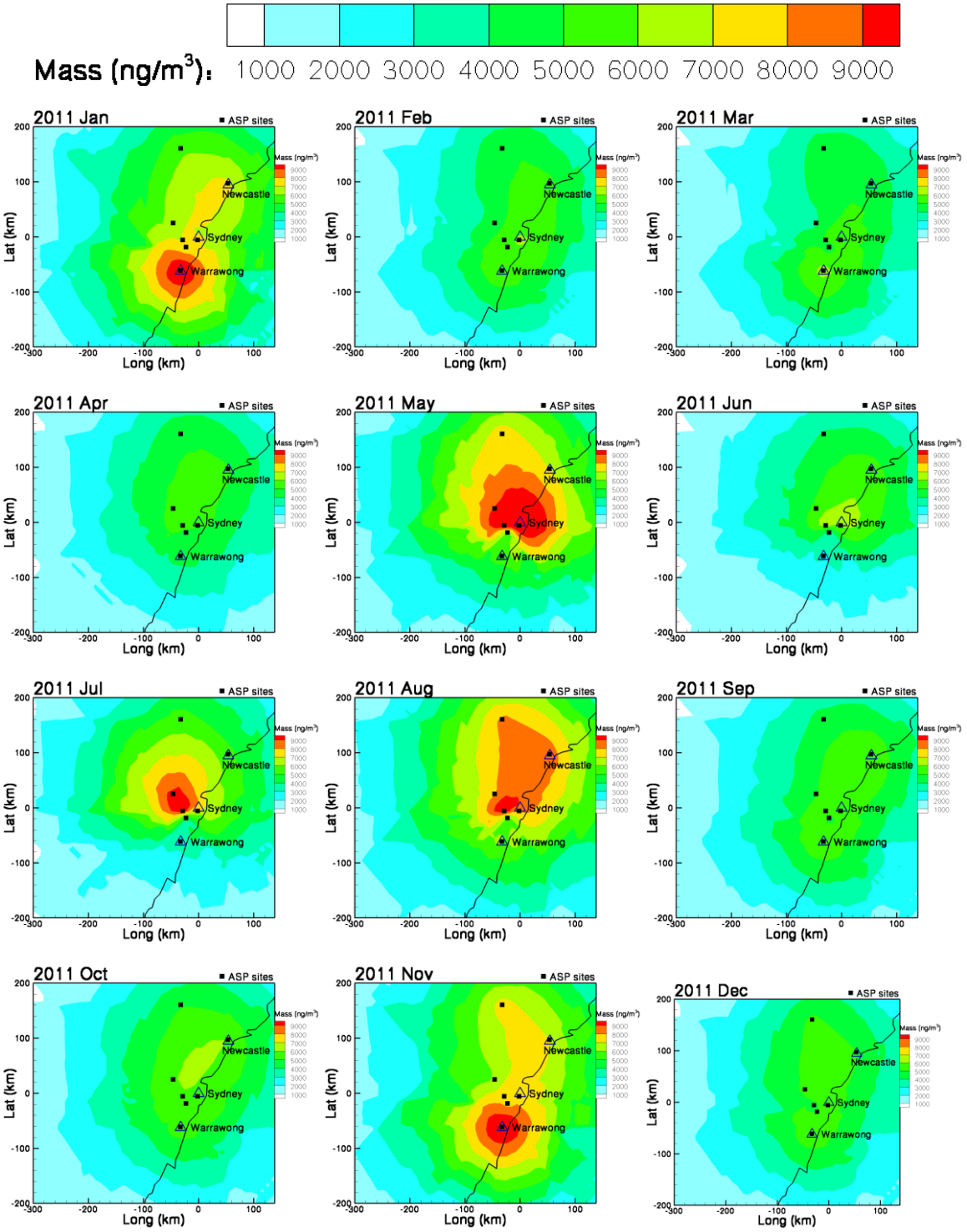

Figure 14: Contour maps of monthly average $PM_{2.5}$ mass concentration for 2011.

Appendix 2: $(NH_4)_2SO_4$ concentration maps

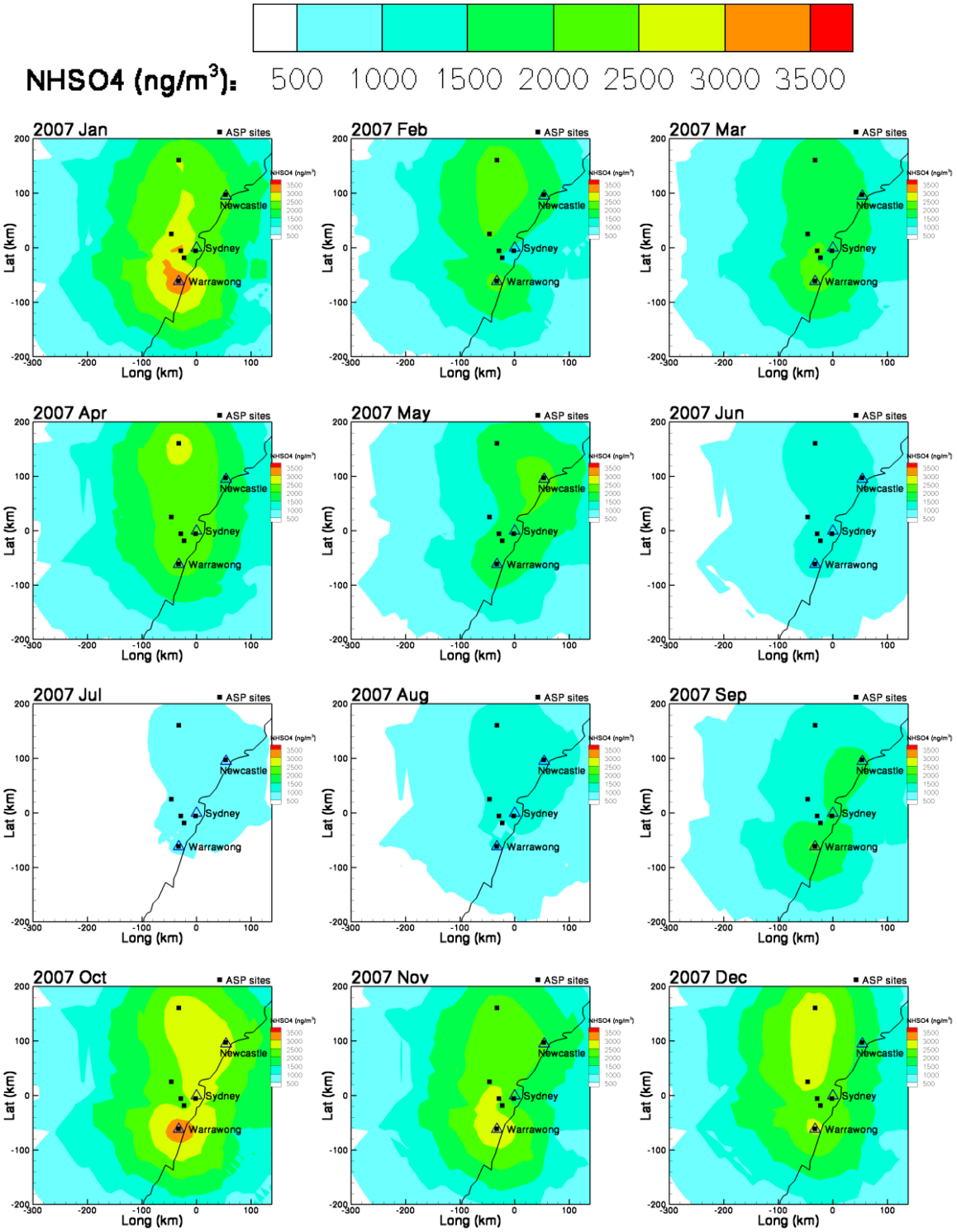

Figure 15: Contour maps of monthly average $(NH_4)_2SO_4$ concentration for 2007.

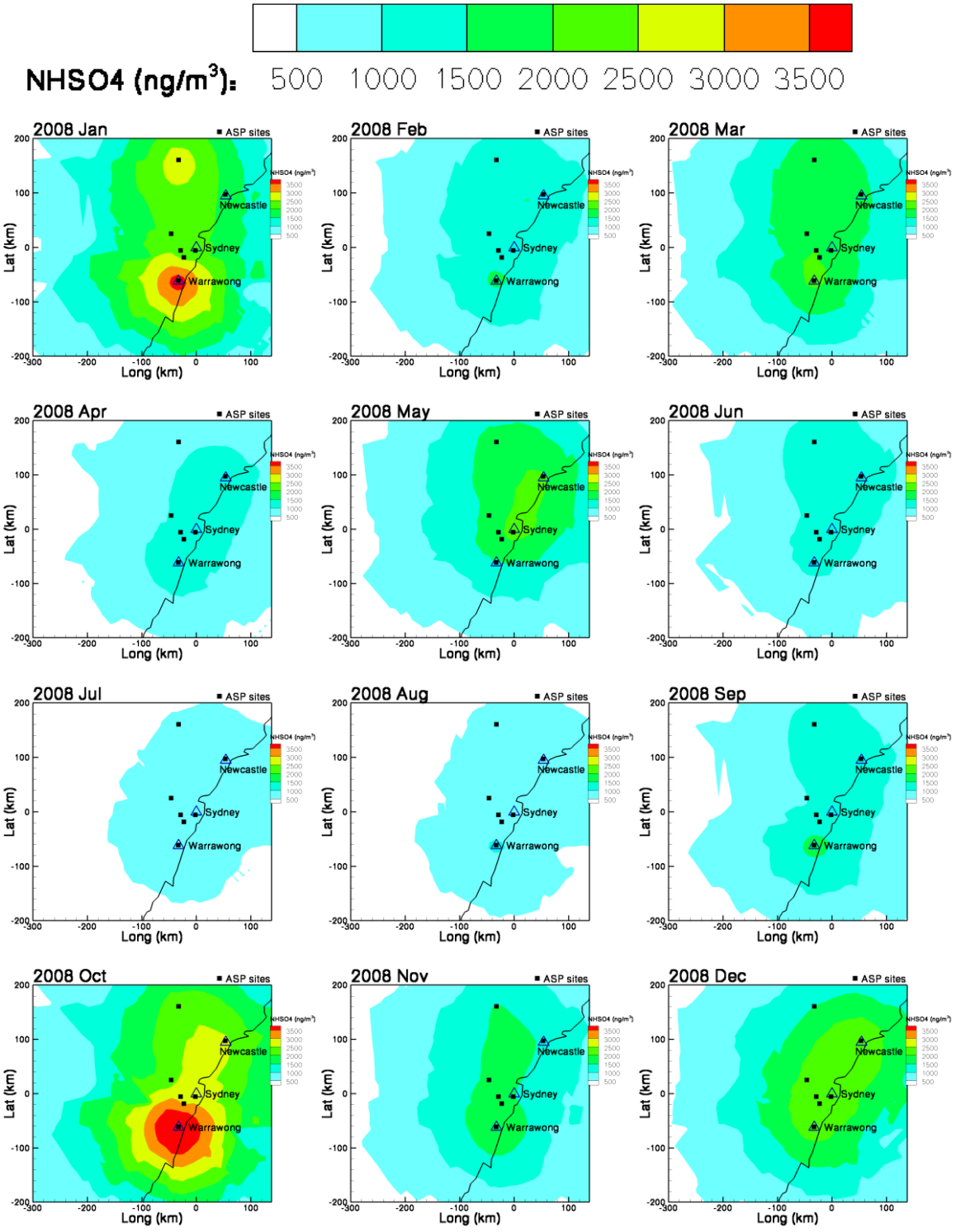

Figure 16: Contour maps of monthly average $(NH_4)_2SO_4$ concentration for 2008.

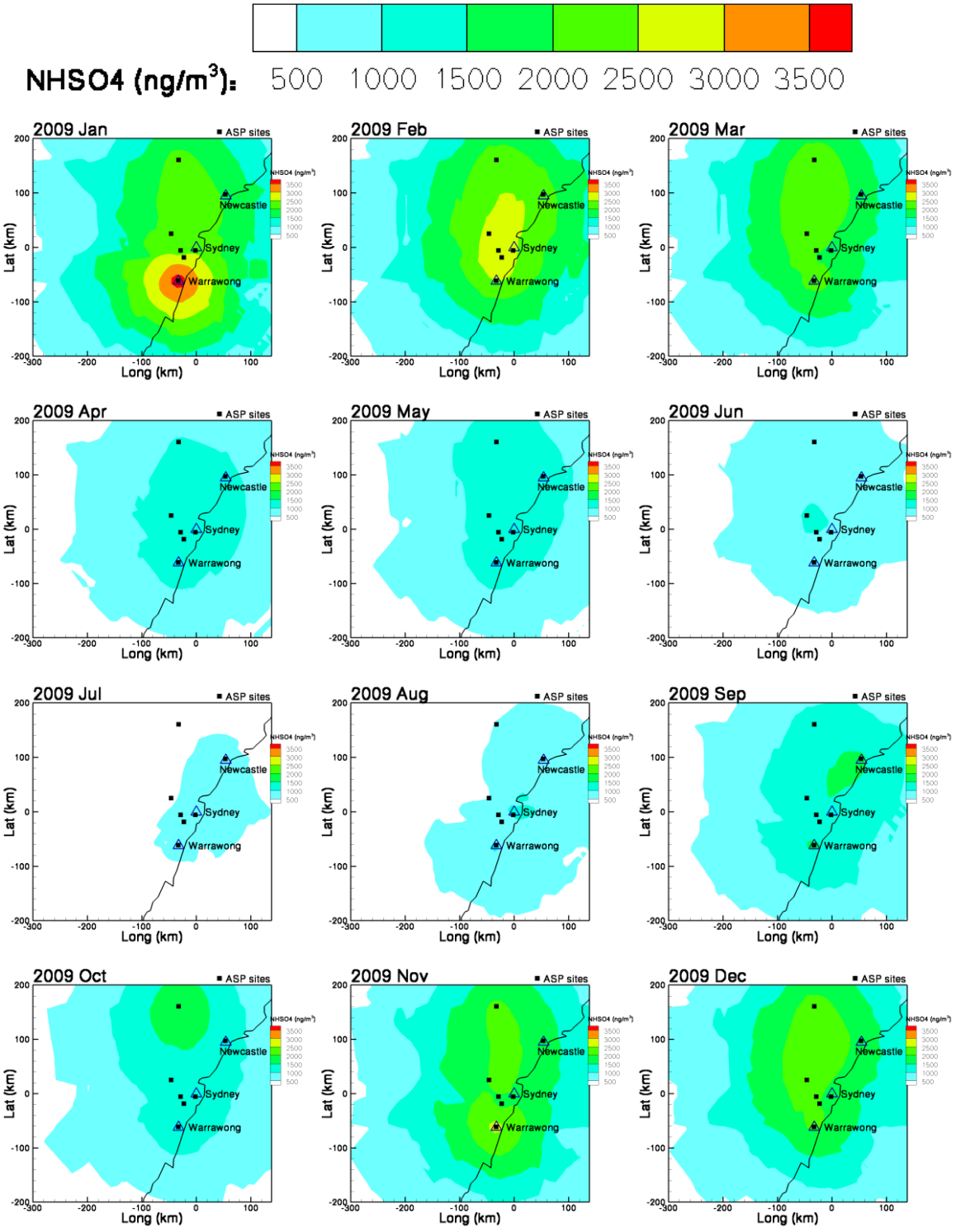

Figure 17: Contour maps of monthly average $(NH_4)_2SO_4$ concentration for 2009.

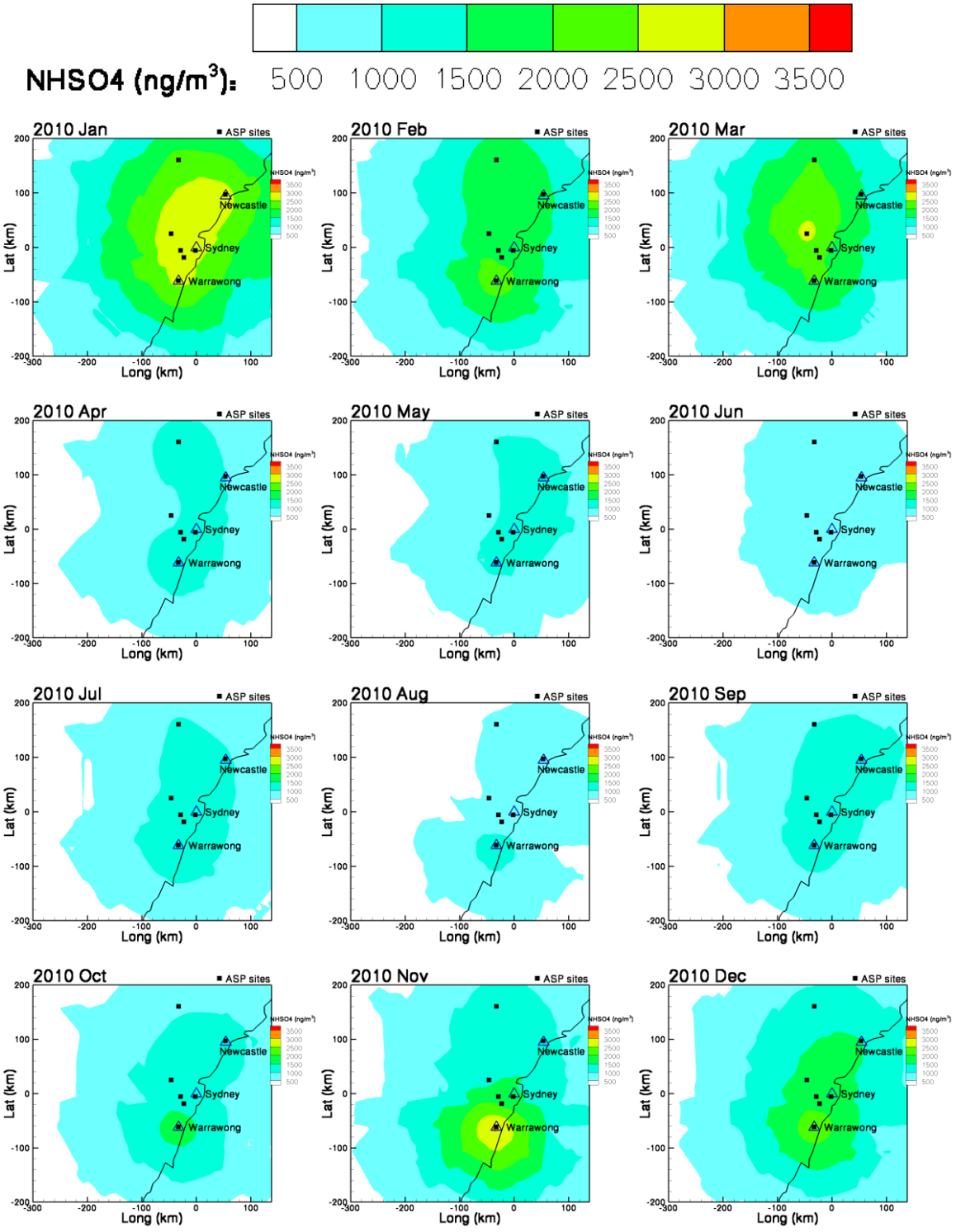

Figure 18: Contour maps of monthly average $(NH_4)_2SO_4$ concentration for 2010.

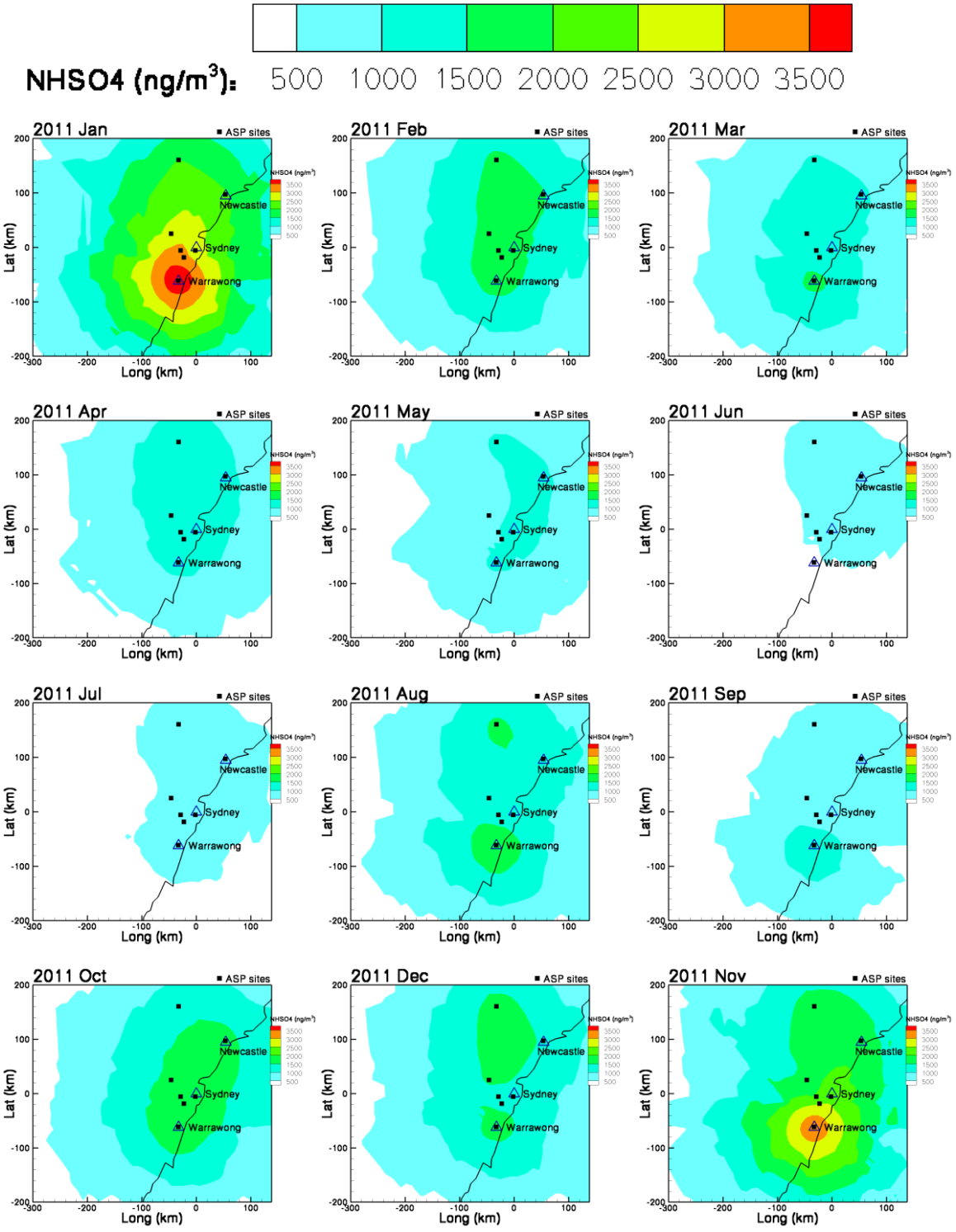

Figure 19: Contour maps of monthly average $(NH_4)_2SO_4$ concentration for 2011.

Appendix 3: BC concentration maps

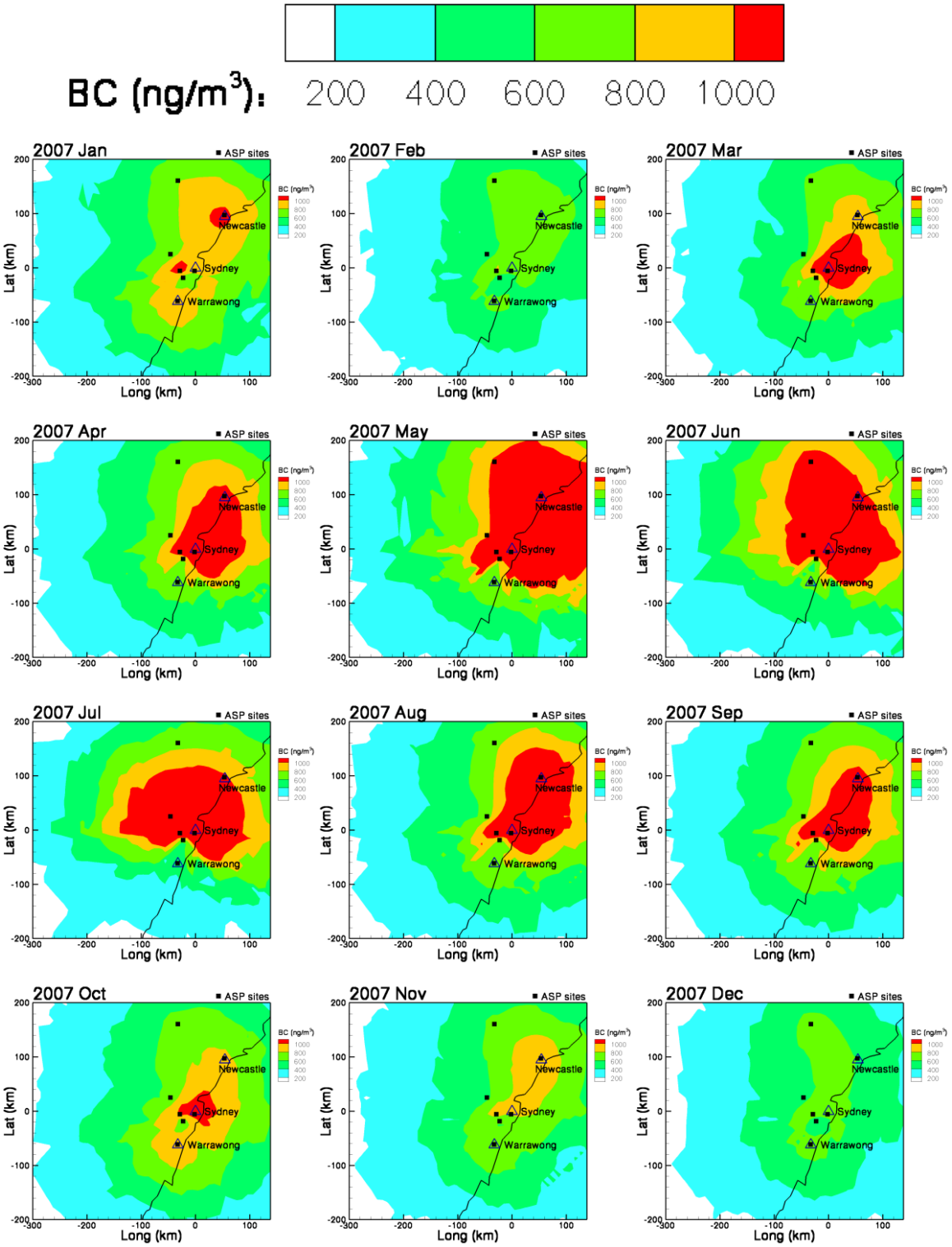

Figure 20: Contour maps of monthly average BC concentration for 2007.

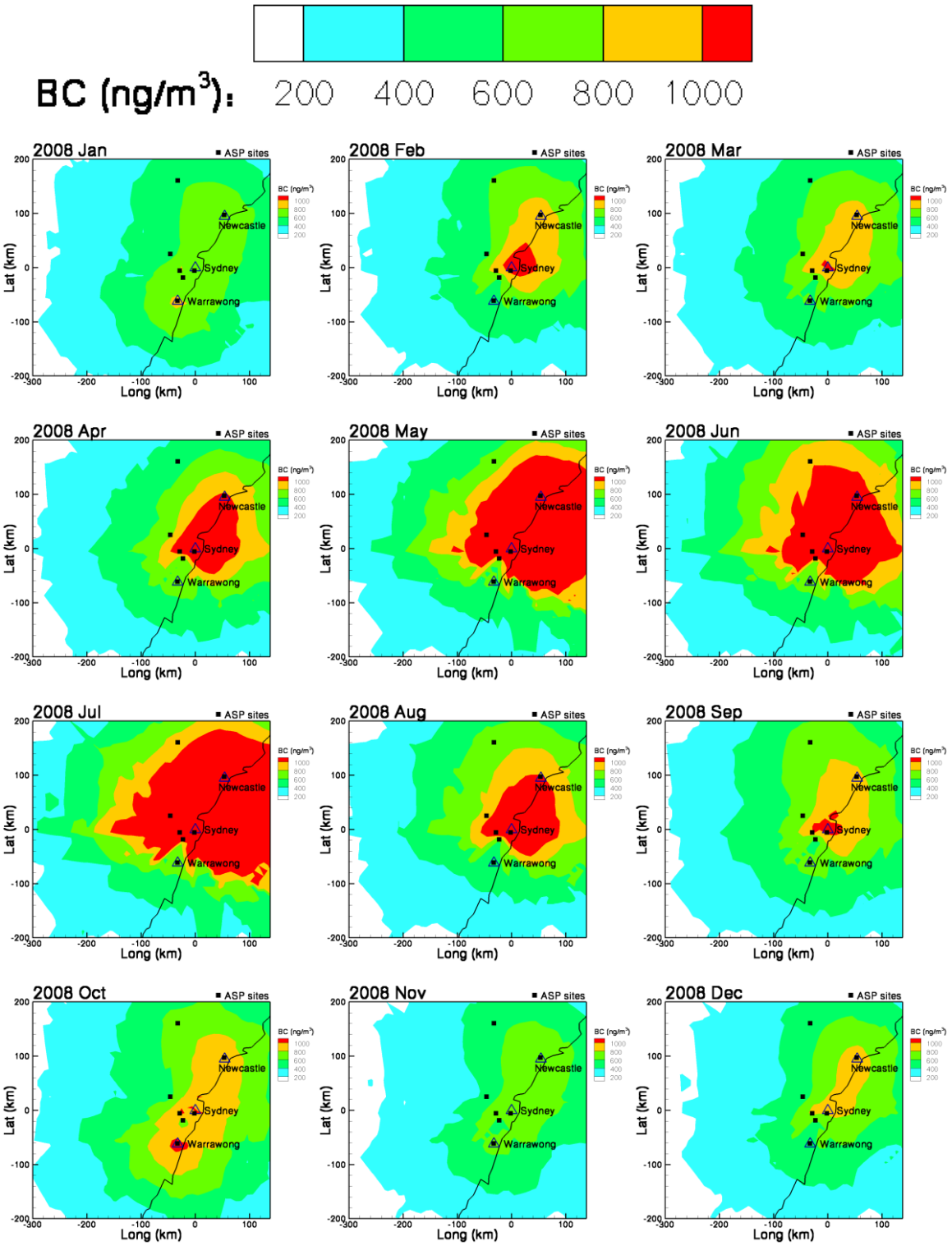

Figure 21: Contour maps of monthly average BC concentration for 2008.

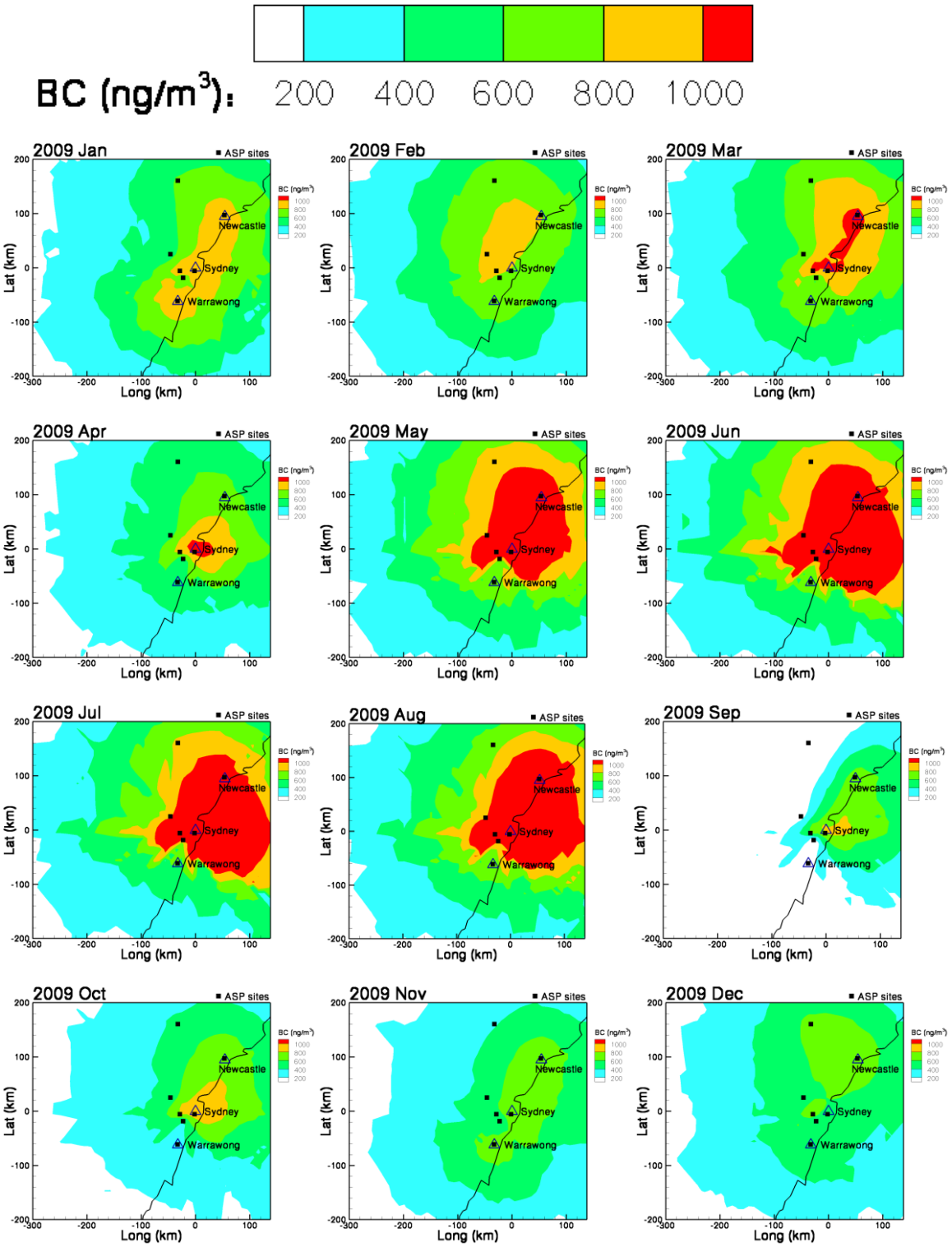

Figure 22: Contour maps of monthly average BC concentration for 2009.

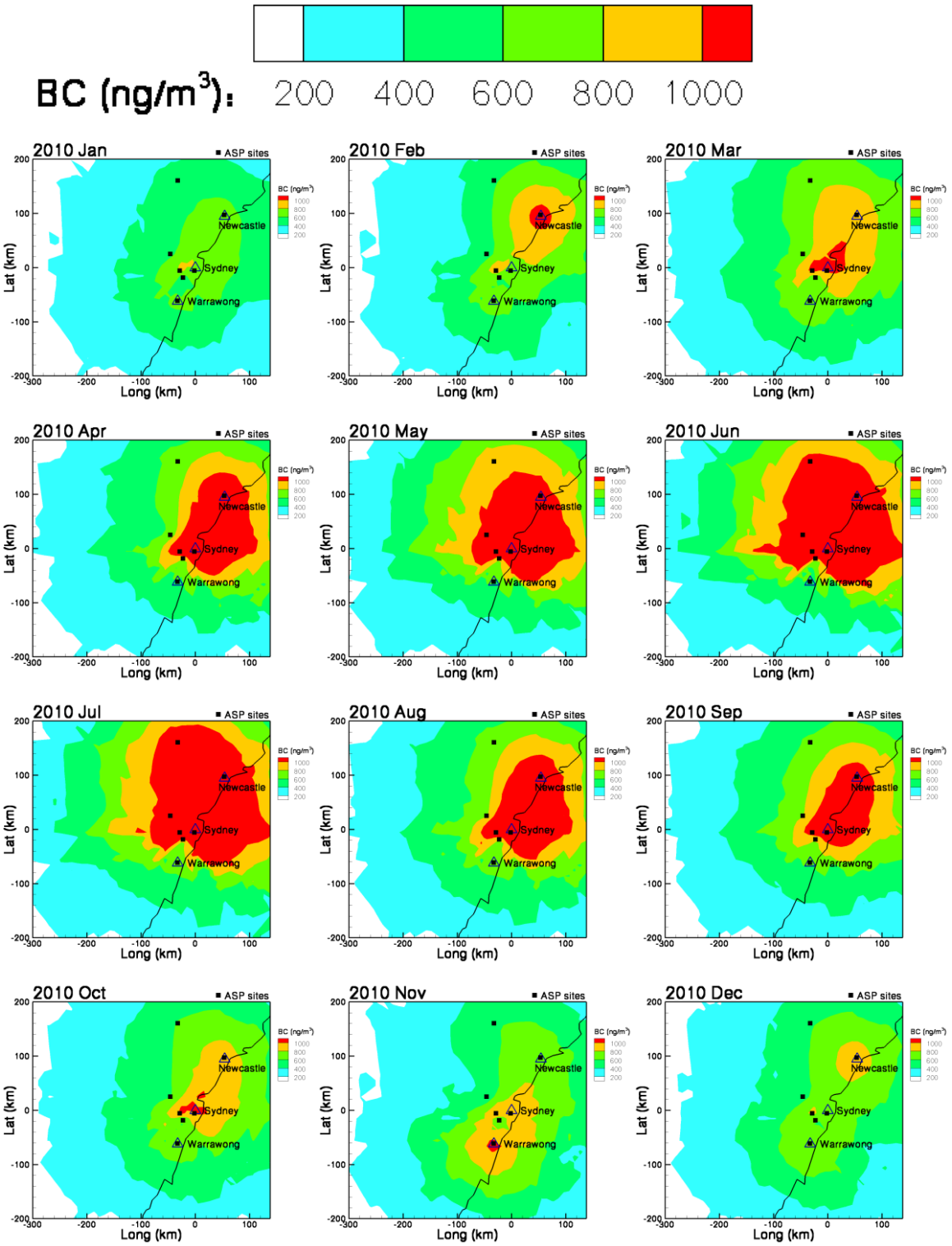

Figure 23: Contour maps of monthly average BC concentration for 2010.

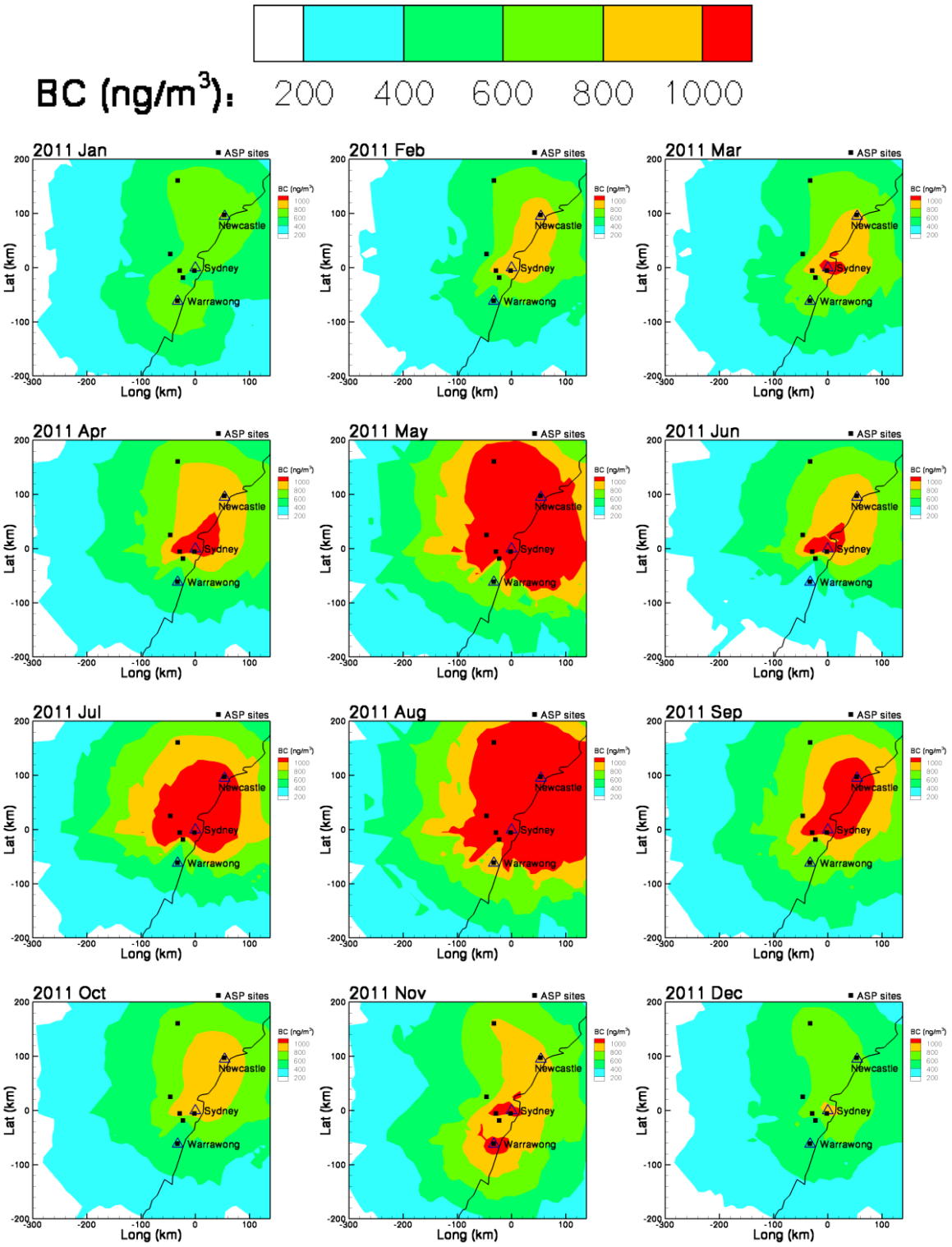

Figure 24: Contour maps of monthly average BC concentration for 2011.

Appendix 4: Salt concentration maps

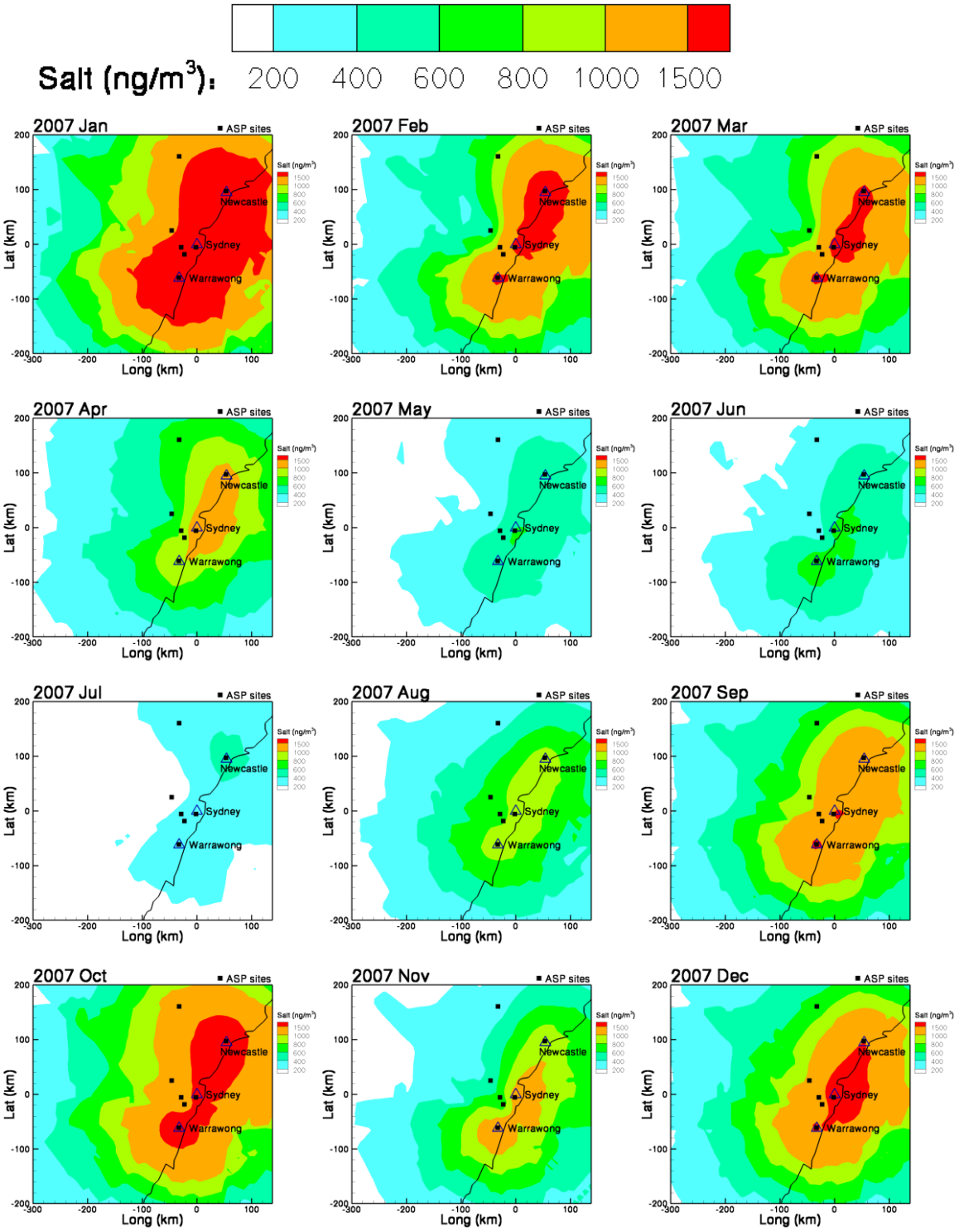

Figure 25: Contour maps of monthly average Salt concentration for 2007.

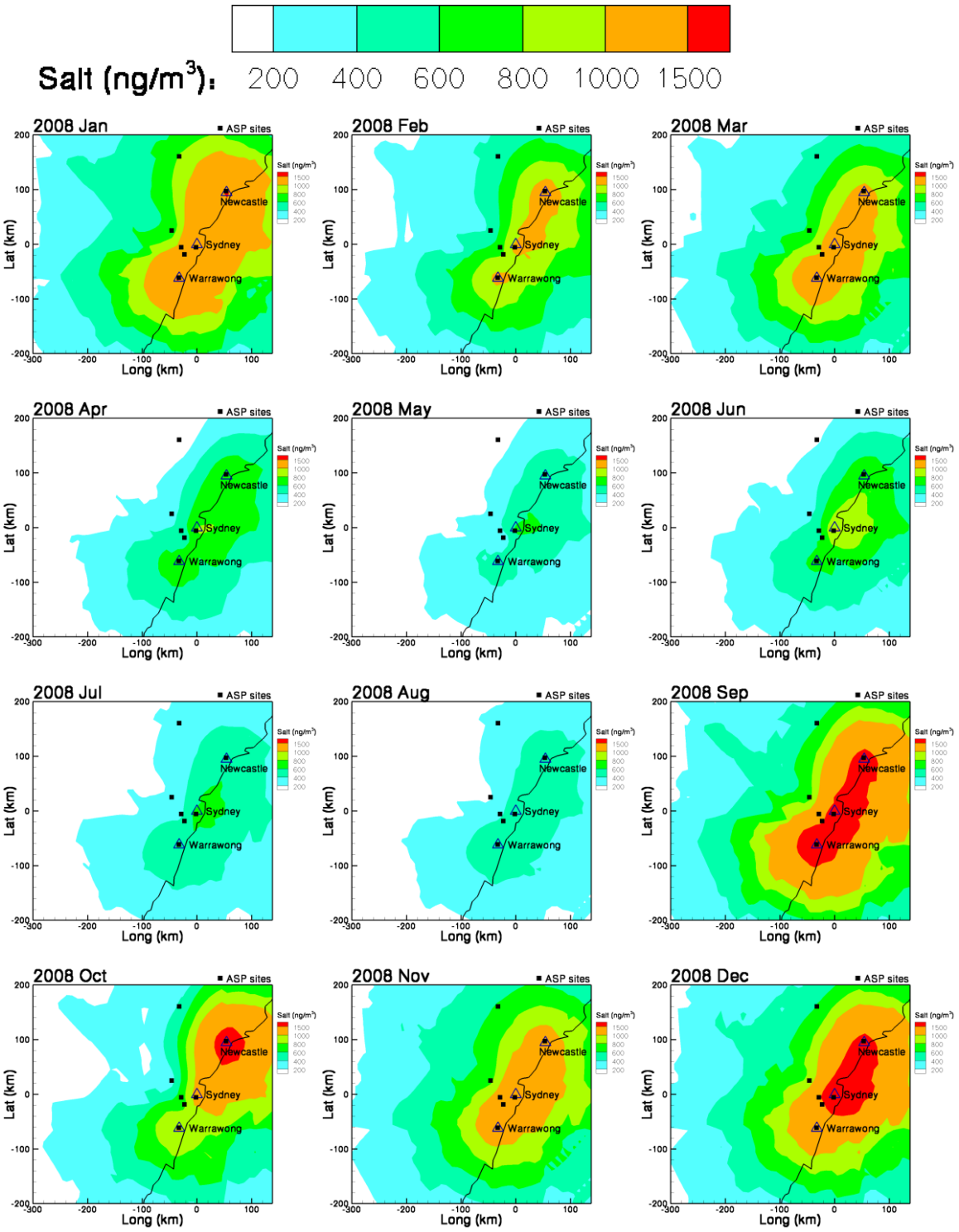

Figure 26: Contour maps of monthly average Salt concentration for 2008.

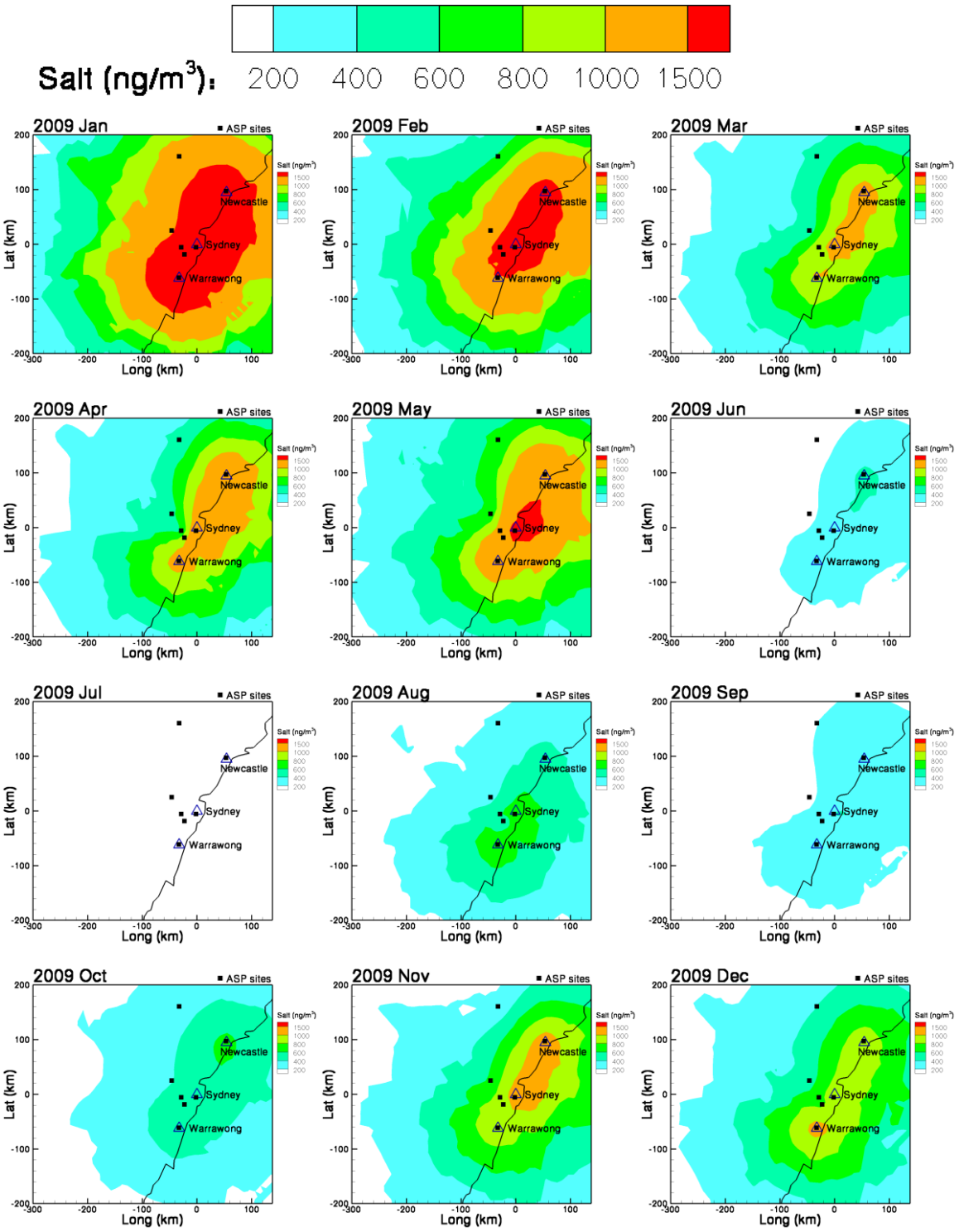

Figure 27: Contour maps of monthly average Salt concentration for 2009.

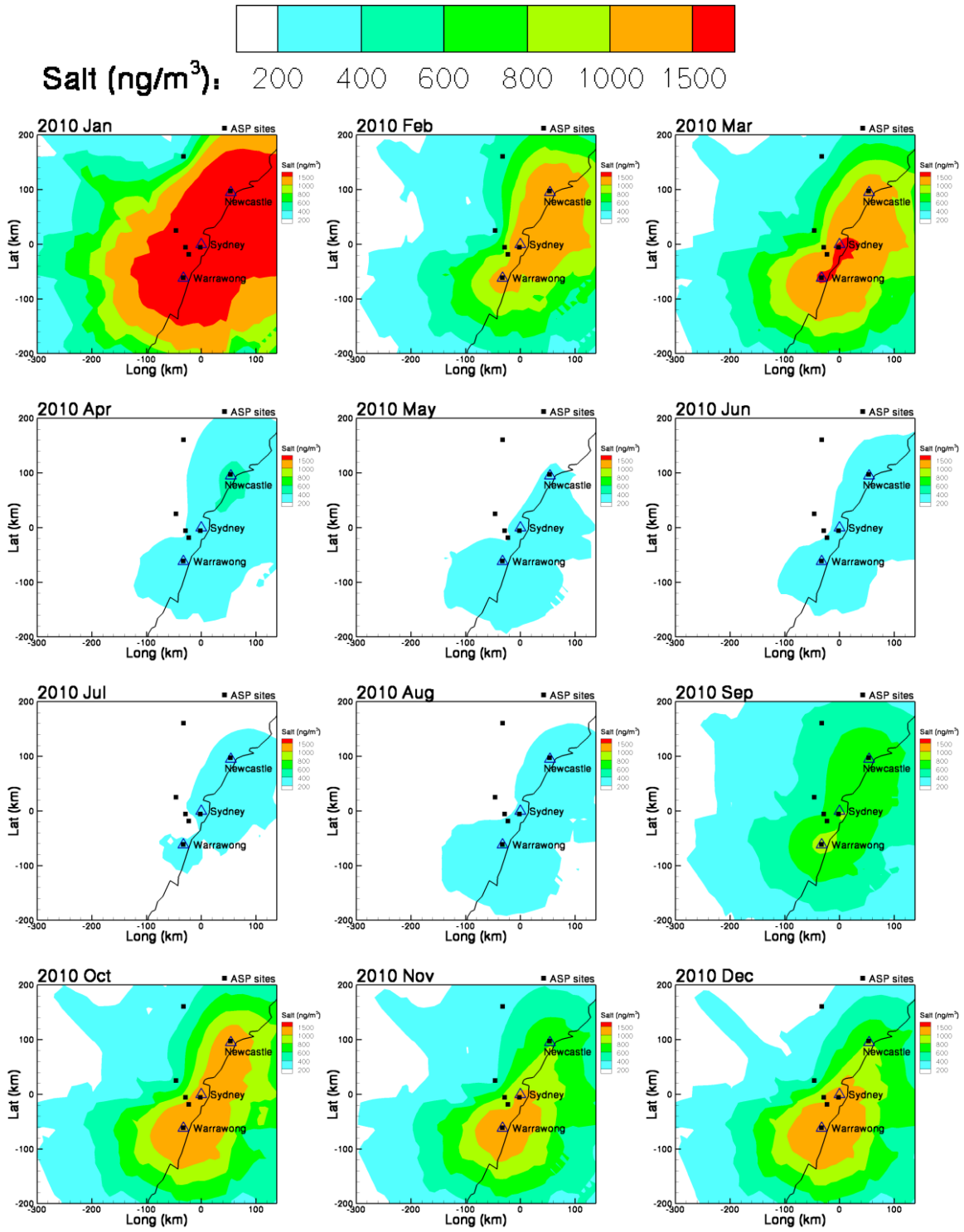

Figure 28: Contour maps of monthly average Salt concentration for 2010.

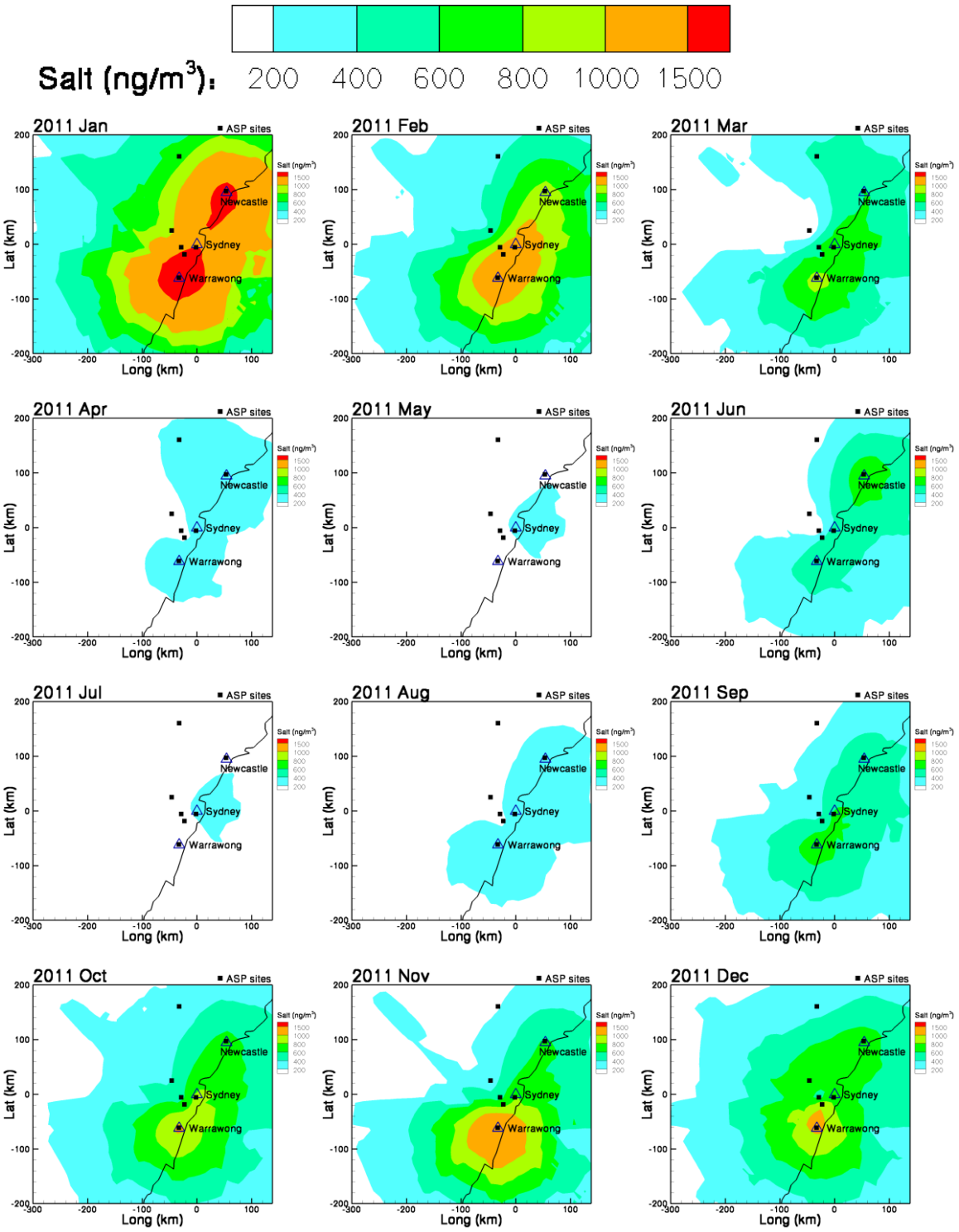

Figure 29: Contour maps of monthly average Salt concentration for 2011.

Appendix 5: K concentration maps

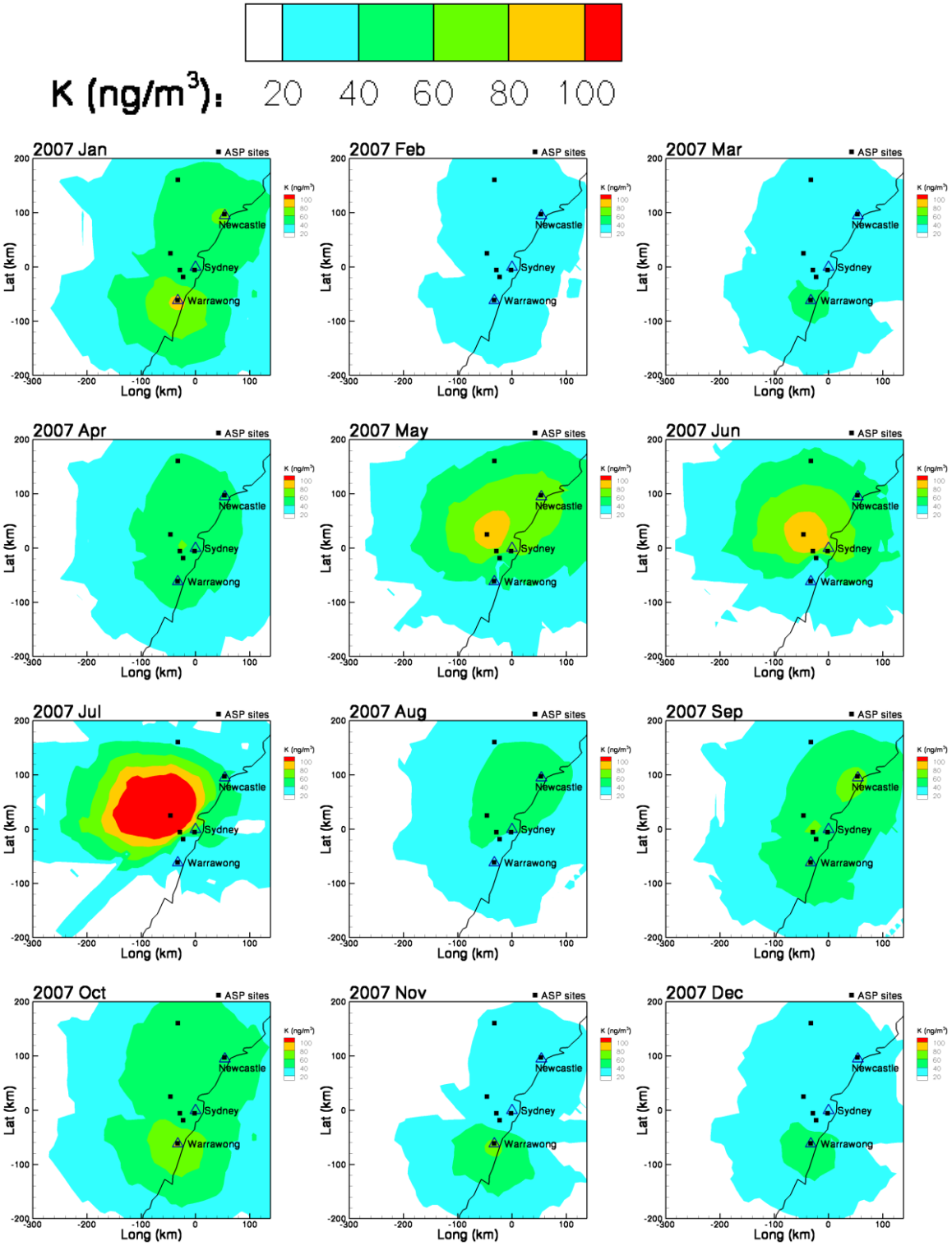

Figure 30: Contour maps of monthly average K concentration for 2007.

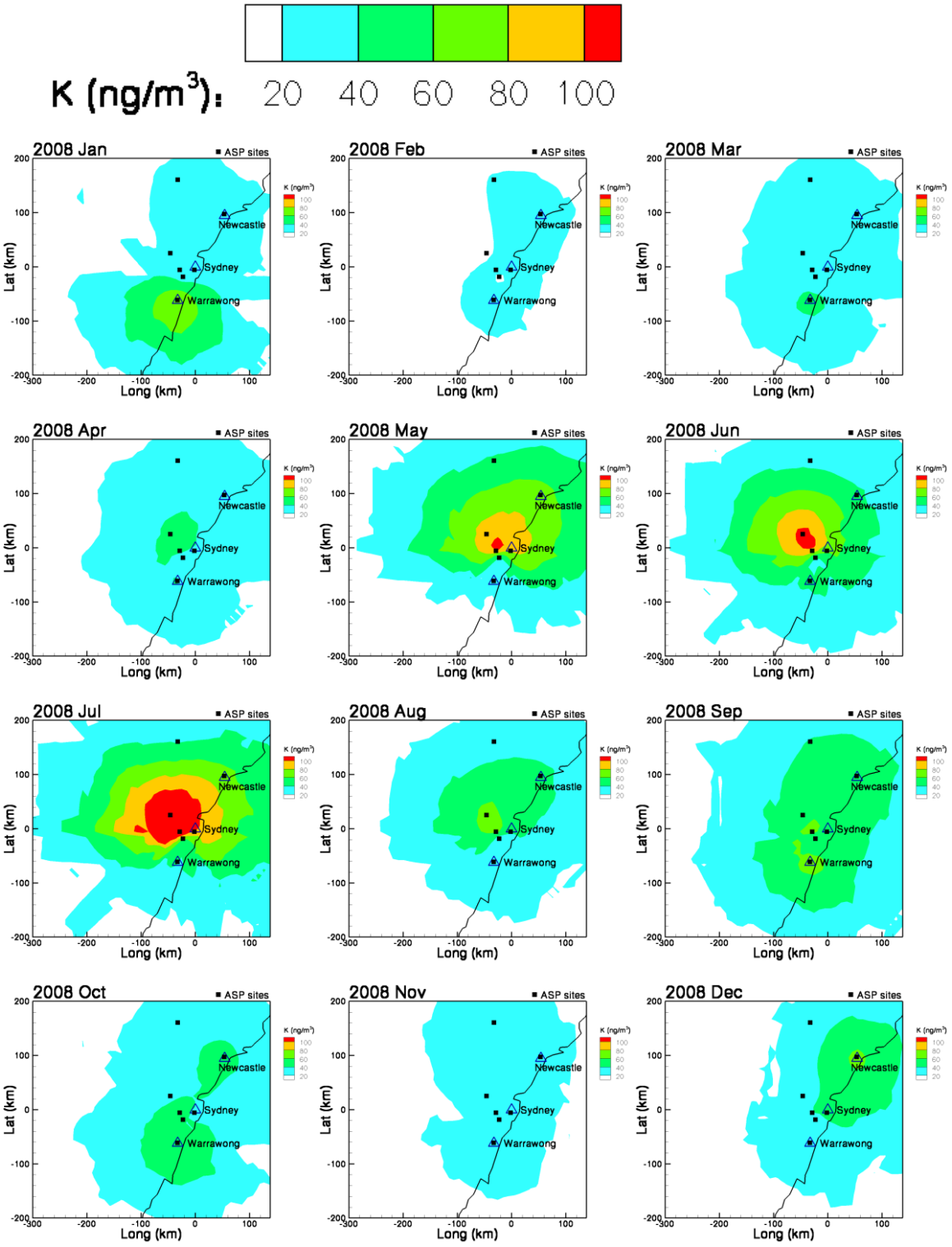

Figure 31: Contour maps of monthly average K concentration for 2008.

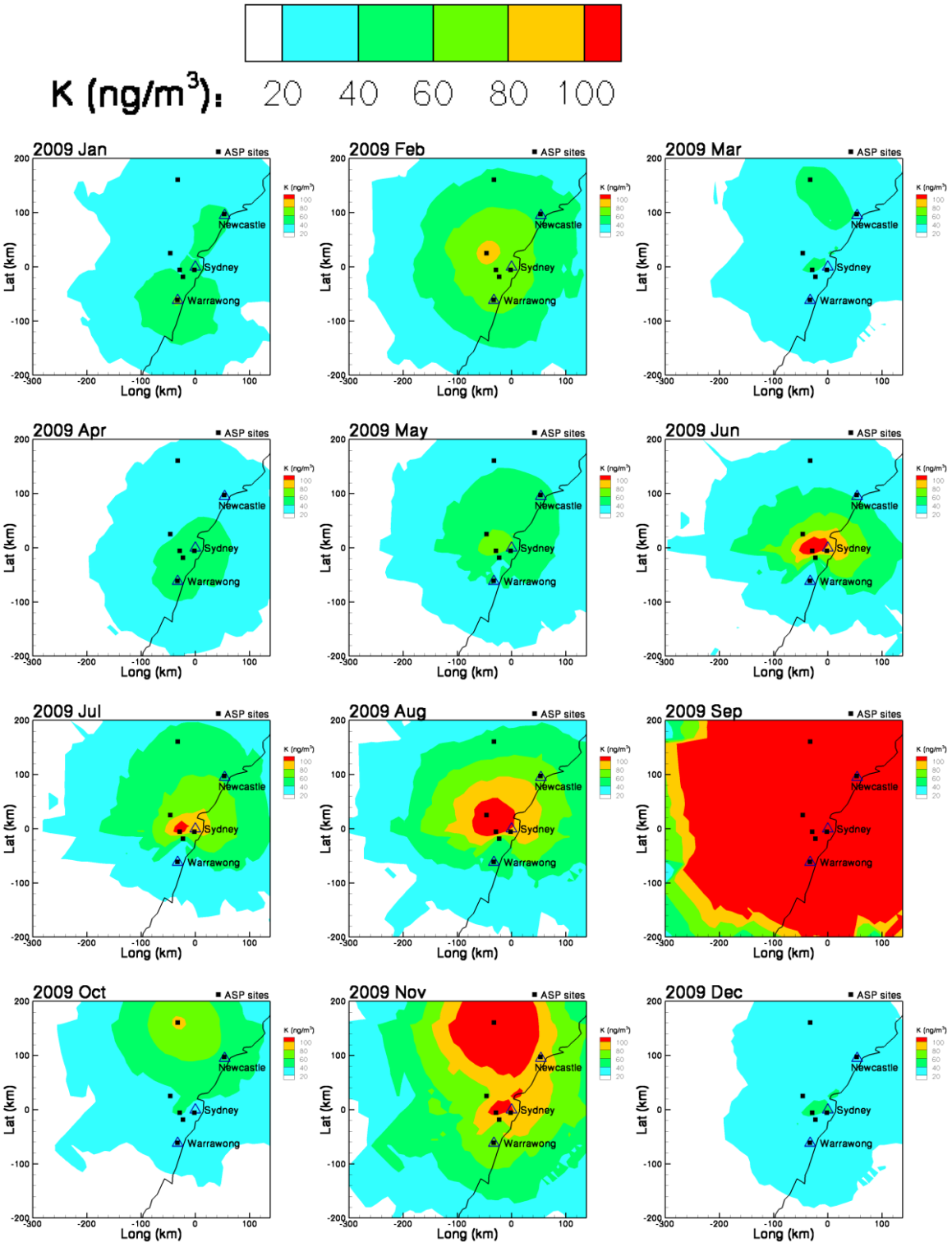

Figure 32: Contour maps of monthly average K concentration for 2009.

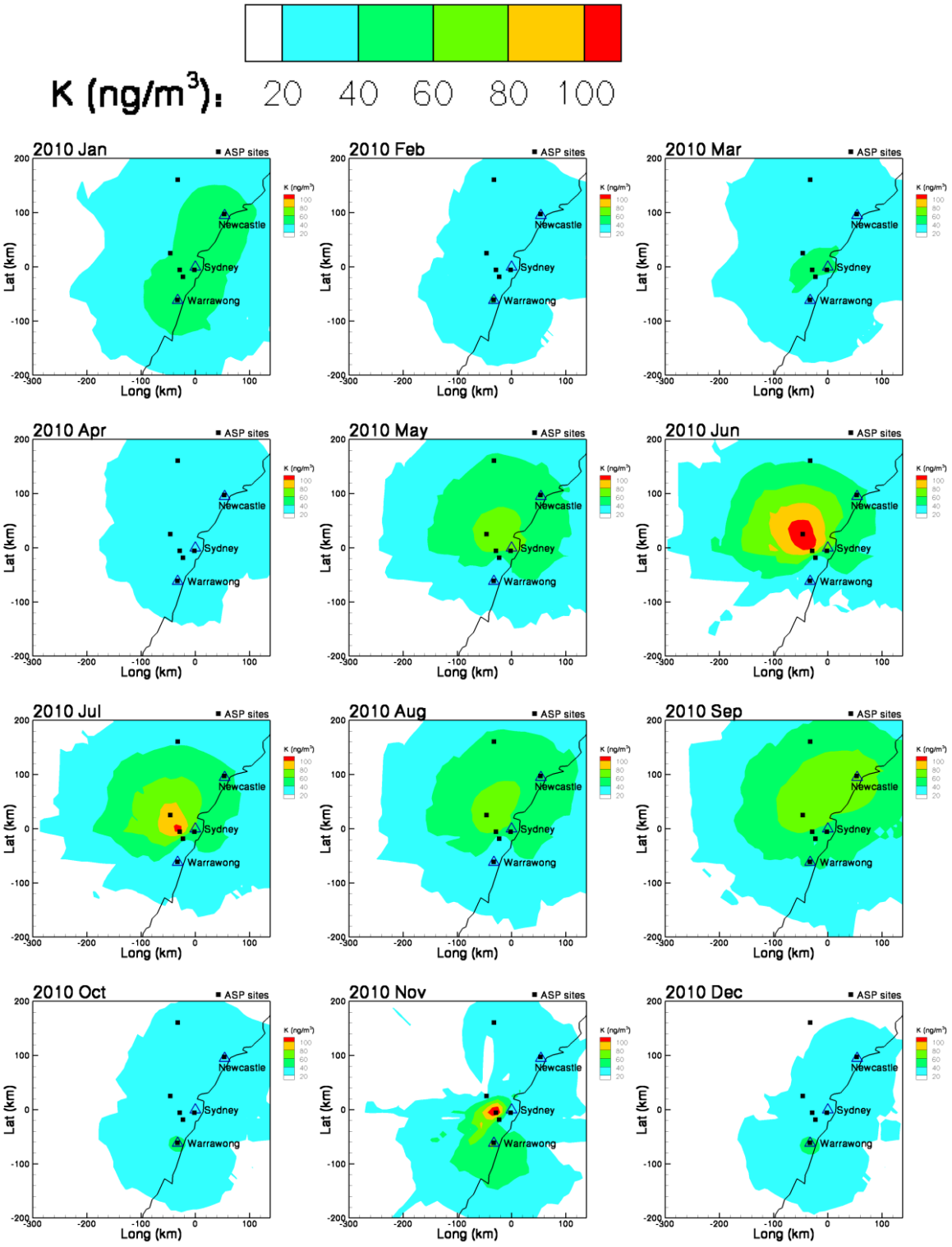

Figure 33: Contour maps of monthly average K concentration for 2010.

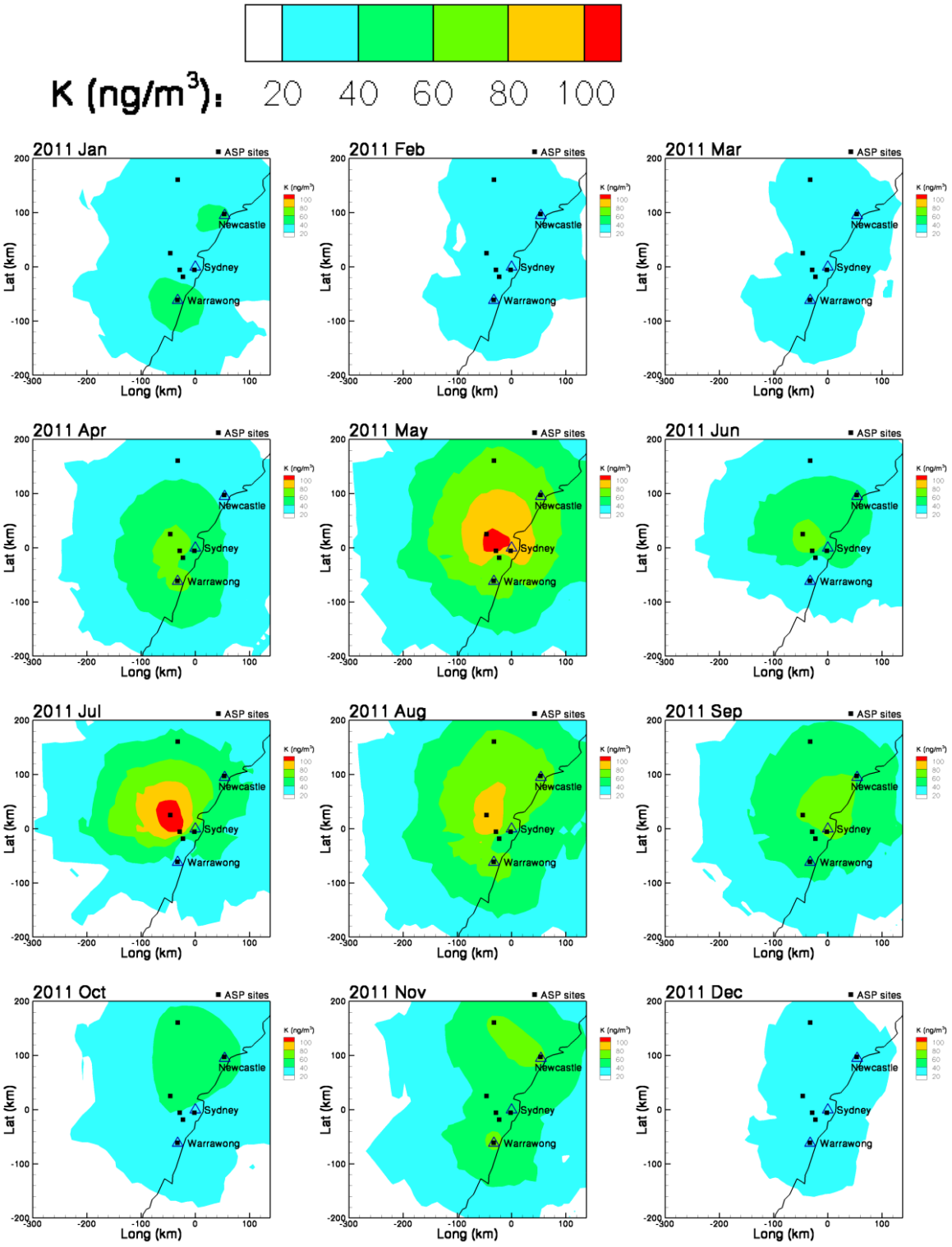

Figure 34: Contour maps of monthly average K concentration for 2011.

Appendix 6: Pb concentration maps

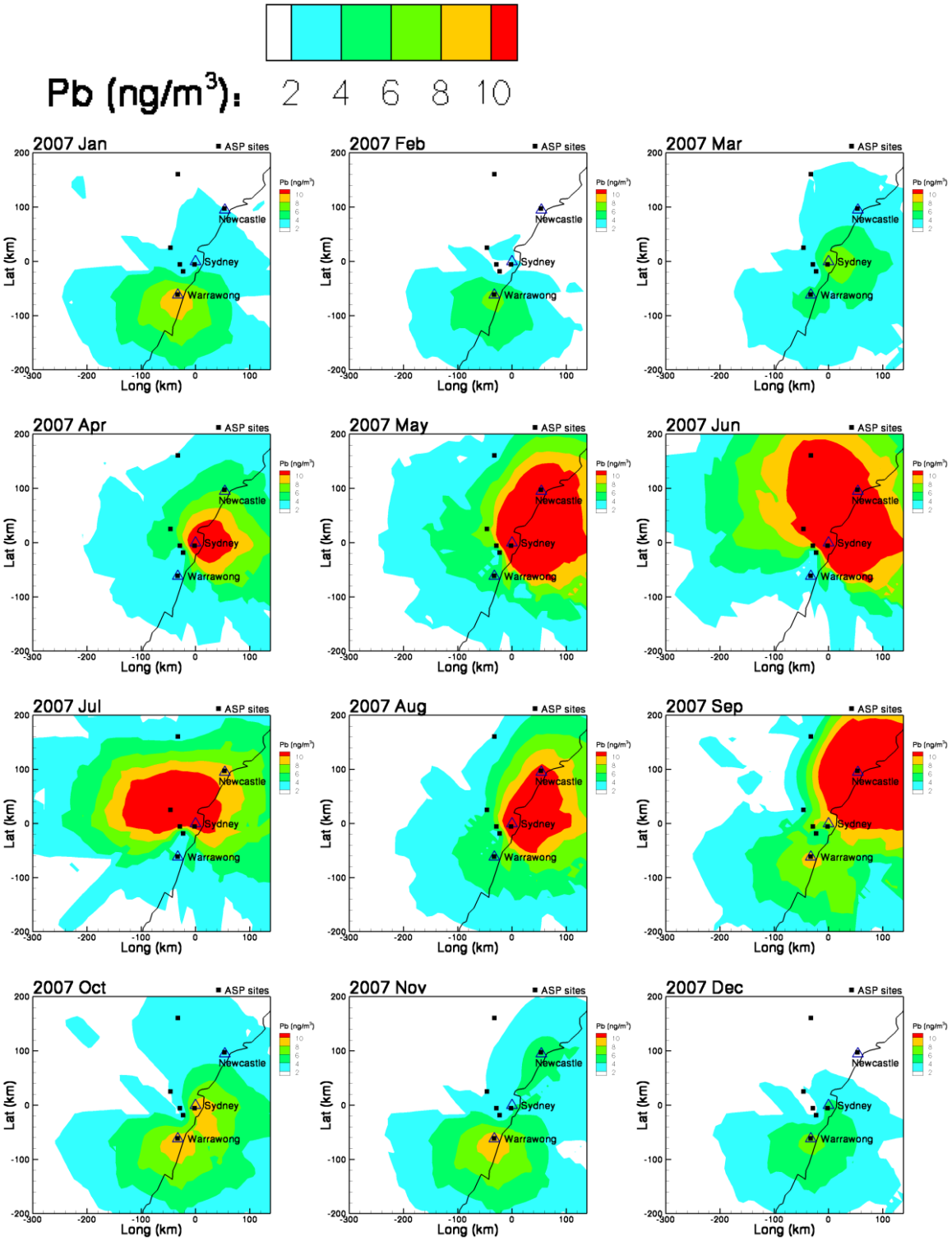

Figure 35: Contour maps of monthly average Pb concentration for 2007.

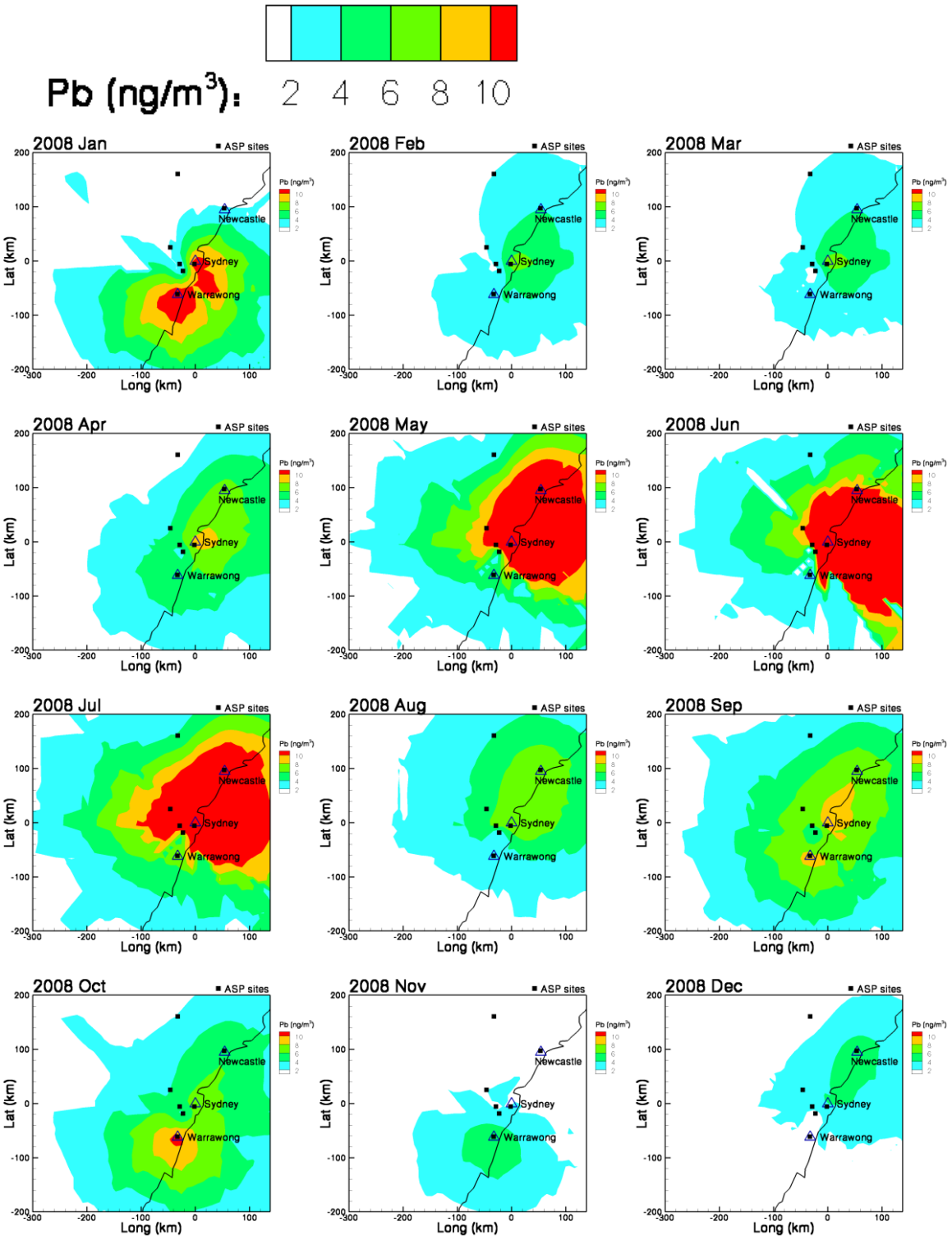

Figure 36: Contour maps of monthly average Pb concentration for 2008.

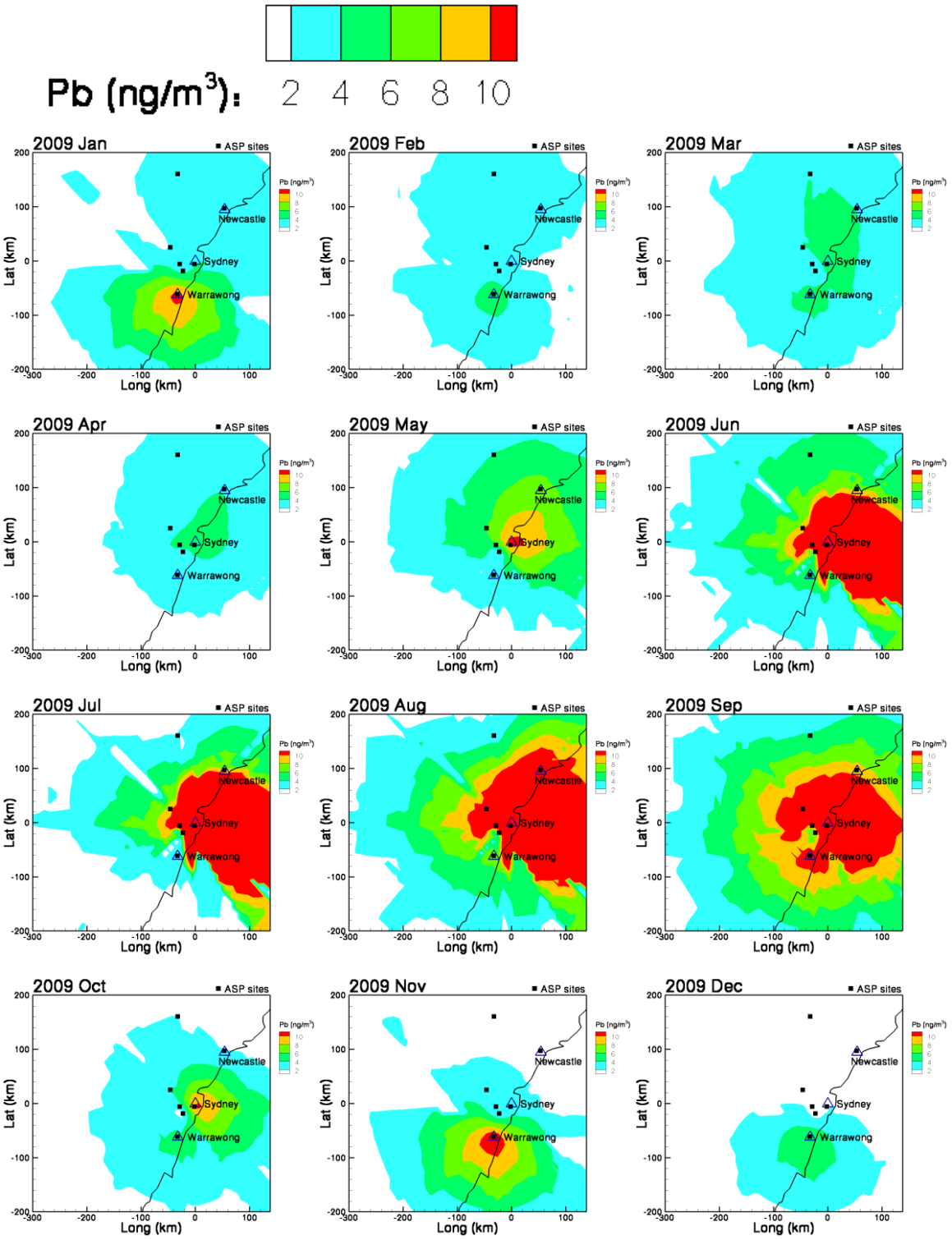

Figure 37: Contour maps of monthly average Pb concentration for 2009.

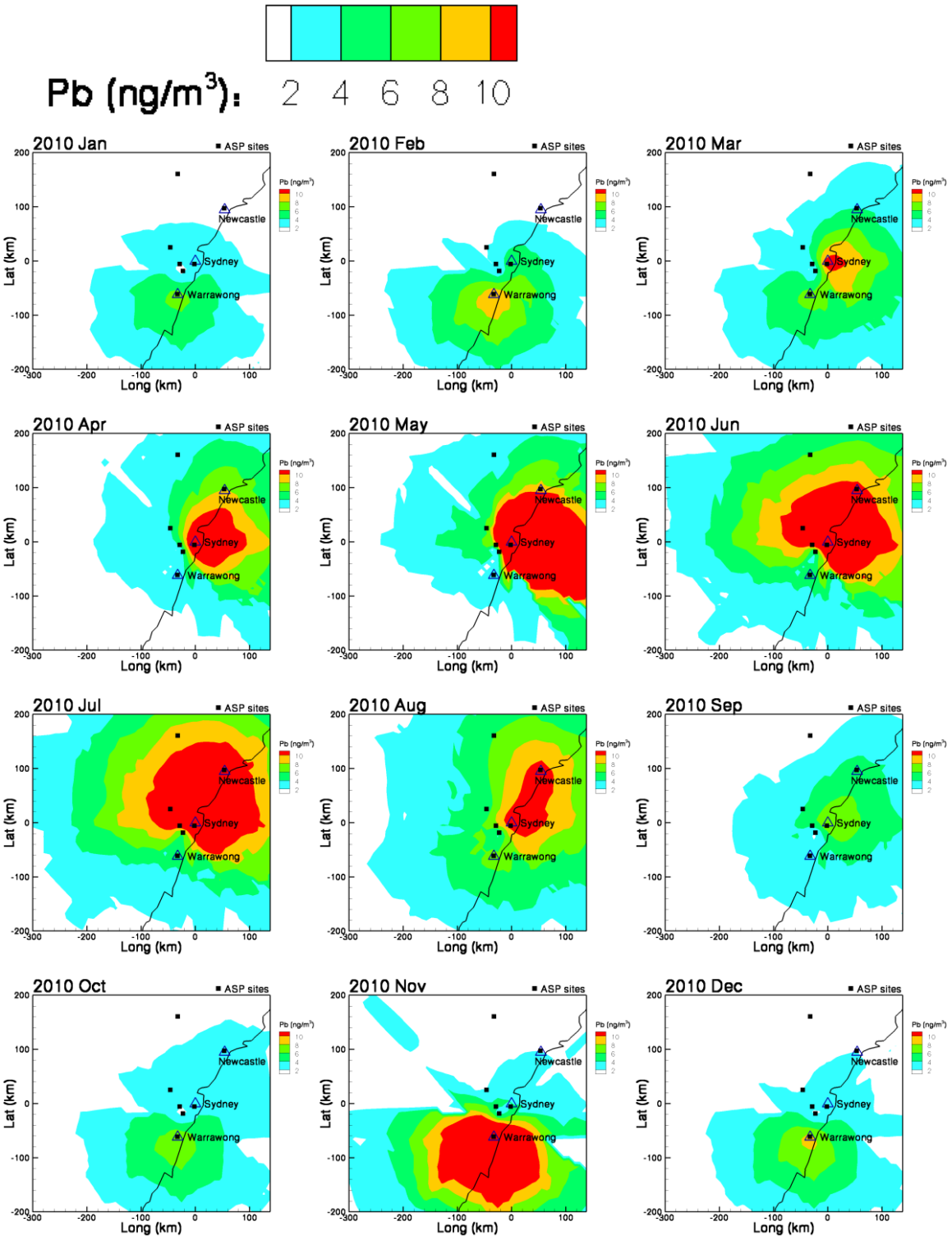

Figure 38: Contour maps of monthly average Pb concentration for 2010.

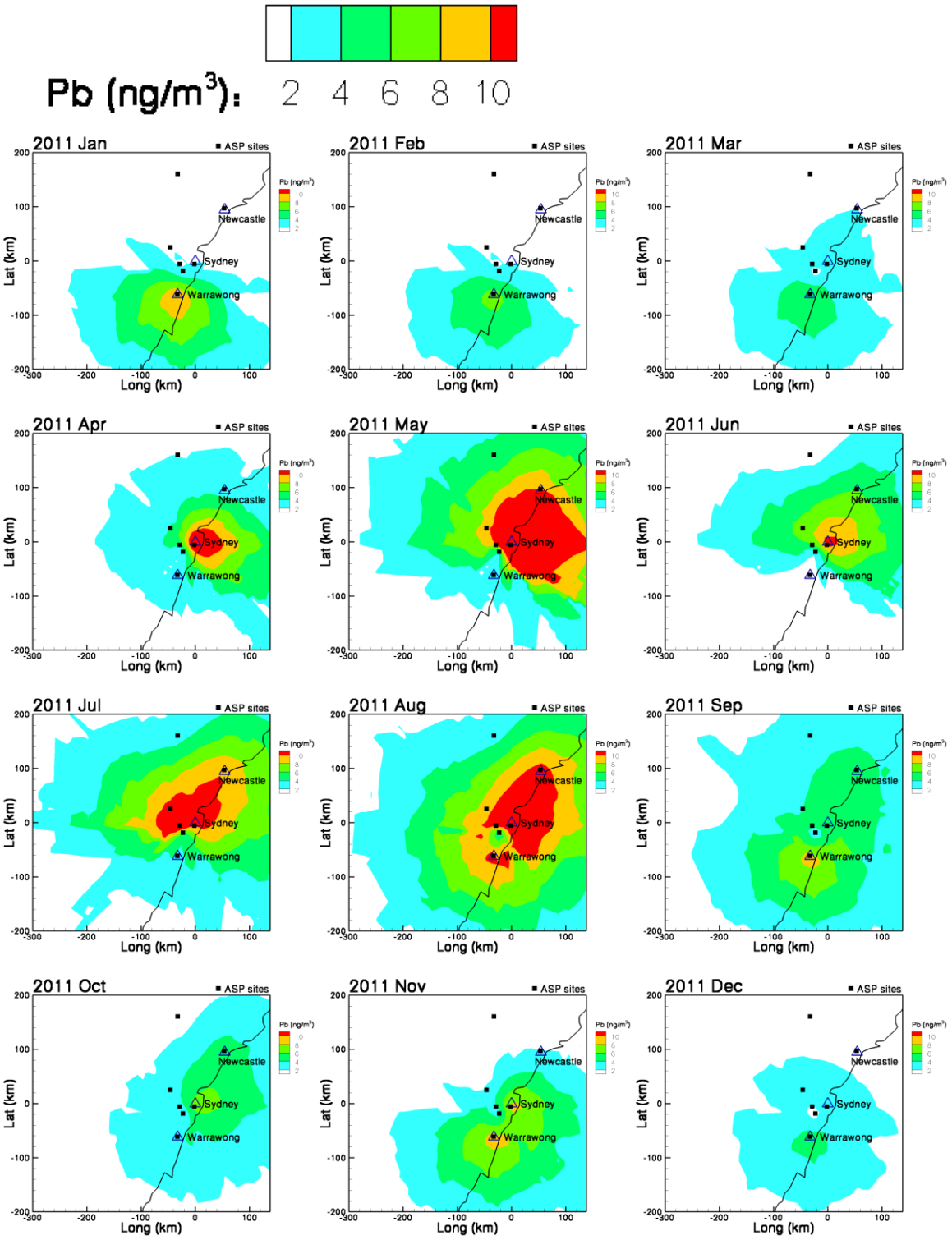

Figure 39: Contour maps of monthly average Pb concentration for 2011.